

Cite this: *Nanoscale*, 2024, **16**, 2713

## Composition, preparation methods, and applications of nanoniosomes as codelivery systems: a review of emerging therapies with emphasis on cancer

Maryam Roostaee,<sup>a</sup> Atefeh Derakhshani, <sup>b</sup> Hadiseh Mirhosseini,<sup>c</sup> Elmira Banaee Mofakham,<sup>d</sup> Sonia Fathi-Karkan, <sup>e,f</sup> Shekoufeh Mirinejad,<sup>g</sup> Saman Sargazi <sup>\*g,h</sup> and Mahmood Barani <sup>\*i</sup>

Nanoniosome-based drug codelivery systems have become popular therapeutic instruments, demonstrating tremendous promise in cancer therapy, infection treatment, and other therapeutic domains. An emerging form of vesicular nanocarriers, niosomes are self-assembling vesicles composed of nonionic surfactants, along with cholesterol or other amphiphilic molecules. This comprehensive review focuses on how nanosystems may aid in making anticancer and antibacterial pharmaceuticals more stable and soluble. As malleable nanodelivery instruments, the composition, types, preparation procedures, and variables affecting the structure and stability of niosomes are extensively investigated. In addition, the advantages of dual niosomes for combination therapy and the administration of multiple medications simultaneously are highlighted. Along with categorizing niosomal drug delivery systems, a comprehensive analysis of various preparation techniques, including thin-layer injection, ether injection, and microfluidization, is provided. Dual niosomes for cancer treatment are discussed in detail regarding the codelivery of two medications and the codelivery of a drug with organic, plant-based bioactive compounds or gene agents. In addition, niogelosomes and metallic niosomal carriers for targeted distribution are discussed. The review also investigates the simultaneous delivery of bioactive substances and gene agents, including siRNA, microRNA, shRNA, lncRNA, and DNA. Additional sections discuss the use of dual niosomes for cutaneous drug delivery and treating leishmanial infections, *Pseudomonas aeruginosa*, and *Mycobacterium tuberculosis*. The study concludes by delineating the challenges and potential routes for nanoniosome-based pharmaceutical codelivery systems, which will be useful for nanomedicine practitioners and researchers.

Received 18th July 2023,  
Accepted 5th December 2023

DOI: 10.1039/d3nr03495j  
[rsc.li/nanoscale](http://rsc.li/nanoscale)

<sup>a</sup>Department of Chemistry, Faculty of Sciences, Vali-e-Asr University of Rafsanjan, Rafsanjan, Iran. E-mail: maryamroostaee3@gmail.com

<sup>b</sup>Department of Tissue Engineering, School of Advanced Technologies in Medicine, Tehran University of Medical Sciences, Tehran, Iran.

E-mail: atefe.drkshani93@gmail.com

<sup>c</sup>Department of Chemistry, Shahid Bahonar University of Kerman, Kerman, Iran. E-mail: mirhoseinihadis@yahoo.com

<sup>d</sup>Department of Nanotechnology and Advanced Materials Research, Materials & Energy Research Center, Karaj, Iran. E-mail: e.banaee@merc.ac.ir

<sup>e</sup>Natural Products and Medicinal Plants Research Center, North Khorasan University of Medical Sciences, Bojnurd, 94531-55166, Iran. E-mail: Soniafathi92@gmail.com

<sup>f</sup>Department of Advanced Sciences and Technologies in Medicine, School of Medicine, North Khorasan University of Medical Sciences, Bojnurd 9414974877, Iran. E-mail: Soniafathi92@gmail.com

<sup>g</sup>Cellular and Molecular Research Center, Research Institute of Cellular and Molecular Sciences in Infectious Diseases, Zahedan University of Medical Sciences, Zahedan, Iran. E-mail: sgz.biomed@gmail.com, shokufemn@gmail.com; Tel: +989103161030

<sup>h</sup>Department of Clinical Biochemistry, School of Medicine, Zahedan University of Medical Sciences, Zahedan, Iran

<sup>i</sup>Medical Mycology and Bacteriology Research Center, Kerman University of Medical Sciences, Kerman 7616913555, Iran. E-mail: mahmoodbarani7@gmail.com

### 1. Introduction

Cancer remains a pressing health concern worldwide, but recent advancements in medicine and other fields show promising strides in revolutionizing treatment approaches.<sup>1–3</sup> Nanotechnology finds diverse applications, from enhancing drug delivery systems in medicine to revolutionizing electronics and materials science for smaller, more efficient devices.<sup>4–6</sup> Over the past few years, nanomedicine has made significant progress.<sup>7,8</sup> Nanoparticles (NPs) are solid colloidal particles with a diameter between 10 and 200 nm and a high surface area-to-volume ratio.<sup>9–11</sup> Due to these characteristics, NPs can assimilate and transport a variety of anticancer agents, including proteins, DNA,<sup>12</sup> RNA,<sup>13</sup> and chemotherapeutic drugs.<sup>14,15</sup> NPs offer precise targeting, improved permeability, a retention effect, the ability to overcome cancer-related drug resistance, increased biocompatibility and stability, the ability to protect normal cells from drug toxicity, the

ability to prolong the half-life of drugs, and the ability to accumulate in tumor tissues over conventional drugs.<sup>7,16,17</sup> Microspheres, erythrocyte immunoglobulins, blood proteins, artificial polymers, liposomes, and niosomes have been used as drug delivery systems.<sup>18,19</sup>

An emerging form of vesicular nanocarriers, niosomes, are self-assembling vesicles composed of nonionic surfactants, along with cholesterol or other amphiphilic molecules.<sup>20,21</sup> These vesicles have a bilayer hydrophobic membrane and a central cavity containing an aqueous phase, allowing them to encase both hydrophilic and hydrophobic substances.<sup>22-24</sup> Niosomes are typically formulated with nonionic surfactants, cholesterol, a charge inducer, and a hydration medium, and are primarily composed of amphiphilic nonionic surfactants with a polar head and nonpolar tail.<sup>25</sup> Nonionic surfactants are more stable, compatible, and less toxic than anionic, cationic, and amphoteric surfactants due to their lack of charge.<sup>26</sup> By inhibiting p-glycoprotein,<sup>27</sup> these agents improve the absorption and delivery of numerous anticancer medications, such as doxorubicin (DOX),<sup>28</sup> curcumin (CUR),<sup>29</sup> morusin,<sup>30</sup> hydrocortisone steroids,<sup>31</sup> HIV-protease inhibitors such as ritonavir,<sup>32</sup> as well as beta-blockers.<sup>33</sup>

Niosome rigidity can be increased by the incorporation of cholesterol into the bilayer structure to decrease membrane permeability, improve membrane stability, and decrease membrane permeability.<sup>34</sup> Electrostatic repulsion inhibits coalescence *via* charge inducers in niosome preparations, contributing to the stability of the niosomes.<sup>35</sup> When niosomes are constructed, dicetyl phosphate and phosphatidic acid are among the most commonly used negatively charged inducers, while stearyl amine and stearylpyridinium chloride are frequently used positively charged inducers.<sup>36</sup> Usually, phosphate buffered saline (PBS) is used for niosome hydration, and their pH changes depending on the solubility of the drug.<sup>23</sup>

Niosomes are divided into three classes with corresponding references based on the size of their compartments.<sup>37</sup> It is possible to categorize niosomes into three types according to the size of their vesicles, such as multilamellar vesicles bigger than 0.05 mm, large unilamellar vesicles bigger than 0.10 mm, and small unilamellar vesicles bigger than 0.025 mm.<sup>38</sup> The production of niosomes involves a variety of techniques, such as the microfluidization technique, reverse phase evaporation technique, ether injection technique, trans-membrane pH gradient (inside acidic) technique, bubble method, supercritical carbon dioxide fluid method, and ball milling technique.<sup>27,39</sup> Niosomes have different physicochemical properties influenced by different variables.<sup>40</sup> The additives and surfactants used in the niosome preparation affect their stability and permeability.<sup>41</sup> By altering how surfactants are assembled into vesicles, the hydration temperature, volume, and duration of niosome hydration can affect their morphologies.<sup>42</sup> A slow release of the medication is caused by difficulty eluting fluid from vesicles, and a rapid release is caused by the mechanical disintegration of vesicles under osmotic stress.<sup>27,37,43</sup>

Nanoniosomes, liposomes, and micelles share a common ground in their role as carriers for drug delivery and therapeutic applications, yet each possesses distinct characteristics. Nanoniosomes exhibit enhanced stability and improved drug encapsulation efficiency compared with conventional liposomes.<sup>44</sup> They harness the advantages of both liposomes and micelles, combining the structural integrity of liposomes with the amphiphilic properties of micelles. While liposomes consist of phospholipid bilayers and micelles form single-layered structures, nanoniosomes strike a balance between these, offering a versatile platform for targeted drug delivery, promising both stability and increased bioavailability.<sup>45</sup> Their innovative nature propels advancements in pharmaceuticals, offering a potential breakthrough in precision medicine and therapeutics.<sup>46</sup>

Numerous advantages of niosomes, such as their capacity to transport multiple drugs at once and reduced systemic toxicity of the drugs in cancer treatments, have prompted researchers to use these nano-carriers for the codelivery of drugs.<sup>47,48</sup> Combination therapy can lead to stronger synergistic effects and greater efficacy.<sup>49</sup> It reduces the risk of severe adverse effects, so it would be more effective than single-agent therapy in inhibiting cancer growth.<sup>50</sup> Niosomes enable the combination of anticancer therapeutics, including chemotherapy, genes, herbal remedies, photodynamic sensitizers, inhibitors of small molecules, classic antineoplastics, and small interfering RNAs (siRNA) in order to block tumor resistance to multiple drug cytotoxicity (MDR) and effectively regulate multiple signaling pathways.<sup>51-57</sup> Using anticancer agents with various mechanisms of action concurrently enhances the therapeutic effects by encompassing more than one mechanism of action, thereby increasing the efficacy of the treatment.<sup>35</sup>

Developing innovative, personalized pharmaceutical products based on novel niosomes will require further research and investigation into formulation, preparation, and modification methods. A concise description of the composition, varieties, and preparation techniques of niosomes is presented in this article, along with examples of how niosomes can be used for targeted delivery, and the simultaneous delivery of several substances. Examples include the codelivery of drug and gene agents, two gene agents, bioactive compounds, and genes, antioxidants, drug niogelosomes, and other therapeutic applications, including in infections, cutaneous drug delivery, and others.

## 2. Classification of niosomal drug delivery systems (DDSSs)

### 2.1. Niosome composition

Niosomes consist of pharmaceuticals, cholesterol or its derivatives, nonionic surfactants, and frequently amphiphilic ions. In niosomes, both hydrophilic and hydrophobic drugs can become confined. Hydrophilic pharmaceuticals are encapsulated in a two-layer hydrophobic zone, whereas hydrophobic

pharmaceuticals are encapsulated in a similar core. Due to its interaction with nonionic surfactants, adding the correct amount of cholesterol to niosomes produces a stable formulation.<sup>58</sup> Niosome formulation essentials include non-ionic surfactants, cholesterol, charge inducers, and a hydration medium.<sup>59</sup> Within the intricate framework of a niosome each component plays a pivotal role, contributing to its functionality and stability. Composed primarily of non-ionic surfactants, cholesterol, and other additives, these components synergize to orchestrate the niosome's properties and applications. The non-ionic surfactants, often the backbone of niosomes, are fundamental in shaping the vesicular structure. They self-assemble to form bilayers, constructing the spherical enclosure that holds aqueous substances within. These surfactants determine crucial aspects such as vesicle size, membrane fluidity, and permeability. Their selection influences the niosome's stability, its ability to encapsulate different payloads like drugs or genetic material, and even its biocompatibility. Cholesterol contributes significantly to the structural integrity of the vesicle. It intervenes in the regulation of membrane fluidity, improving stability by modulating the packing of surfactant molecules. By reducing permeability and enhancing rigidity, cholesterol aids in controlling the drug release kinetics and preventing the premature leakage of encapsulated compounds. Additional additives, including stabilizers or modifiers, can further refine niosome properties. These substances might augment vesicle stability, enhance drug-loading capacity, or promote targeted delivery by altering surface properties. Modifiers like polyethylene glycol (PEG) can confer stealth characteristics, reducing immune recognition and prolonging the circulation time in the body.<sup>46,60</sup>

**2.1.1 Non-ionic surfactants.** Non-ionic surfactants are necessary for the formation of niosomes, which are vesicles used to encapsulate drugs. These surfactants have several advantageous characteristics, such as natural biodegradability, amphiphilicity, nonimmunogenicity, and biocompatibility. Non-ionic surfactants lack an electrical charge, unlike cationic, anionic, and amphoteric surfactants, rendering them less toxic, compatible, and stable. The additives, composition, size, surface charge, and lamellarity of niosomes are dependent on the specific types and combinations of non-ionic surfactants employed. Tween (20, 40, 60, and 80) and Span (60, 40, 20, 85, and 80) are examples of frequently utilized non-ionic surfactants. Non-ionic surfactants interact with cellular surfaces with less hemolysis and irritation compared with other surfactant varieties. They play a crucial role in the formulation of numerous physical, chemical, and organic compounds. Due to their efficacy in producing synthetic lipid bilayer membranes, surfactants and phospholipids, including non-ionic surfactants, are frequently used in the administration of medications. The ability of non-ionic surfactants to inhibit p-glycoprotein is an essential characteristic. This inhibition can improve the absorption and targeting of certain drugs, such as steroids (e.g., hydrocortisone), anticancer drugs (e.g., daunorubicin, morusin, DOX, and CUR), cardiovascular medications (e.g.,

beta-blockers, digoxin), and HIV protease inhibitors (e.g., ritonavir). Therefore, non-ionic surfactants substantially improve the therapeutic efficacy of these medications.<sup>27</sup> Table 1 lists the various varieties of non-ionic surfactant utilized in the production of niosomes.<sup>61</sup>

The production of bilayer vesicles is affected by the critical packing parameter (CPP), the hydrophilic-lipophilic balance (HLB) scale, the constituents' chemical composition, and the gel liquid transmission temperature. Longer alkyl chains increase the entrapment efficiency of non-ionic surfactants. The Tween series of surfactants containing cholesterol and an extended alkyl chain with an enlarged hydrophilic moiety has the highest entrapment efficiency for water-soluble medications. The HLB value of a surfactant is essential for controlling drug entrapment in the vesicle it creates. The CPP value of a surfactant can be calculated using the length and volume of the non-polar component and the head area of the polar component. Fig. 1 illustrates how CPP parameters can be used to predict the type of vesicle that will form, and eqn (1) can be used to calculate the CPP. It is anticipated that the surfactant property will play a significant role in the *in vivo* performance of these drug delivery methods, as it is a crucial component that affects the physicochemical properties of niosomes, such as particle size, two-layer strength, drug release, and consistency.<sup>62</sup>

$$CPP = \frac{V}{I_c \times a_0} \quad (1)$$

**Table 1** Examples of the various types of surfactant used to develop niosomes<sup>61</sup>

Non-ionic surfactants	Surfactant examples
<b>Alkyl esters:</b>	
(i) Spans <sup>a</sup>	Span 20, Span 40, Span 60, Span 65, Span 80, Span 85
(ii) Tweens <sup>b</sup>	Tween 20, Tween 60, Tween 60, Tween 40, Tween 80, Tween 85
<b>Alkyl ethers:</b>	
(i) Alkyl glycerol ethers	Hexadecyl diglycerol ether
(ii) Polyoxyethylene glycol alkyl ethers (Brij)	Brij30, Brij52, Brij72, Brij76, Brij78
Crown ethers	Bola
<b>Alkyl amides:</b>	
(i) Glycosides	C-glycoside derivative surfactant
(ii) Alkyl polyglucoside	Octyl-decyl polyglucoside
<b>Fatty alcohols or fatty acids</b>	
(i) Fatty alcohols	Stearyl alcohol, acetyl alcohol, myristyl alcohol
(ii) Fatty acids	Stearic acid, palmitic acid, myristic acid
Block copolymer: (i) Pluronic	Pluronic L64, Pluronic 105
Lipidic components:	
cholesterol	
l- $\alpha$ -Soya phosphatidyl choline	
Charged molecule:	
Negative charge	Dicetyl phosphate, phosphatidic acid, lipoamino acid, dihexadecyl phosphate
Positive charge	Stearyl amine, stearyl pyridinium chloride

<sup>a</sup> Sorbitan fatty acid esters. <sup>b</sup> Polyoxyethylene sorbitan fatty acid esters.

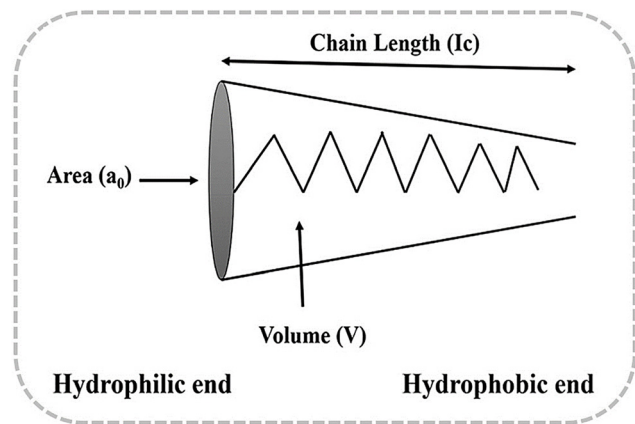


**Fig. 1** Schematic representation of an amphiphile:  $a_0$ , hydrophilic head group area;  $v$ , hydrophobic chain volume; and  $I_c$ , hydrophobic chain length. Reproduced from ref. 63 with permission from [MDPI], copyright [2022].

where  $I_c$ : non-polar group's critical length,  $V$ : non-polar group's volume,  $a_0$ : polar head group's area.

**2.1.2. Cholesterol.** Cholesterol is an oily steroid that is primarily used to produce niosomes and is essential for the rigidity, flexibility, and permeability of cellular membranes. In addition to being necessary for niosome synthesis, cholesterol also influences several of their characteristics.<sup>64</sup> By stabilizing the membrane by incorporating cholesterol into the bilayer structure of the niosomes, the permeability of the cell membrane is reduced, and the entrapment effect of the niosomes is typically enhanced. It is well known that cholesterol prevents the transition of the niosomal system from the gel to the liquid phase, resulting in niosomes that are less likely to escape. Because a substantial quantity of cholesterol affects the permeability or penetration of niosomal vesicles, cholesterol is only sparingly introduced to niosomes. This demonstrates how free-dried niosomes can be rehydrated by enhancing the permeability, encapsulation efficiency (EE), and rigidity. Cholesterol promotes vesicle stability when combined with low HLB surfactants, and when the HLB value exceeds 6, it aids in the formation of bilayer vesicles. In addition, the addition of cholesterol increases the formulation's viscosity and, consequently, its rigidity.<sup>35</sup>

**2.1.3. Charge inducers.** A charged molecule is introduced to the formulation of niosomes in order to prevent aggregation. To increase the stability of niosomes through electrostatic repulsion and prevent coalescence, charge inducers are added to the formulation. Most frequently employed as negatively charged compounds are lipoamino acid, dihexadecyl phosphate, phosphatidic acid, and dicetyl phosphate (DCP). Similarly, positively charged inducers utilized in niosomal compositions consist of stearyl pyridinium chloride and stearyl amine (STR).<sup>65</sup> Concentrations of charged inducers between 2 and 5 mole percent are permissible but concentrations greater than this can inhibit the formation of nio-

somes. In order to create a niosome, the charged molecule must be present at a concentration of 2.5% to 5% by mole.<sup>66</sup>

**2.1.4. Hydration medium.** The hydration medium is one of the most significant factors in niosome formation. Phosphate buffer saline is the most commonly used hydration medium in the production of niosomes. The solubility of the substance within the capsule determines the pH of the hydration environment.<sup>67</sup>

## 2.2. Types of niosome based on the lamellarity

As previously mentioned, niosomes may be categorized into three groups depending on their size or the number of lamellar layers [*i.e.*, small unilamellar vesicles (SUVs), large unilamellar vesicles (LUVs), and multilamellar vesicles (MLVs) variants] (Fig. 2). SUVs range from 10 to 100 nm in length. Typically, they are created from multilamellar vesicles utilizing sonication, French press extrusion, homogenization, or microfluidic techniques. In addition, they are more susceptible to fusion and aggregation and thermodynamically less stable than other types of niosome. Their entrapped volume is modest, and their drug-loading capacity for hydrophobic substances is modest.<sup>68</sup> The lengths of the large unilamellar vesicles range from 100 to 3000 nm. Unilamellar vesicles with a colossal diameter and a single bilayer membrane are found on LUVs. Compared with other types, this vesicle contains a greater quantity of drugs. This type of niosome has a high aqueous/lipid section ratio, allowing for the extremely efficient use of membrane lipids to encapsulate greater quantities of bioactive compounds.<sup>69</sup> Typically, reverse-phase evaporation and ether injection techniques are used to produce these vesicles. LUVs are more advantageous than MLVs due to their predictable drug release rates, ability to encapsulate more water-

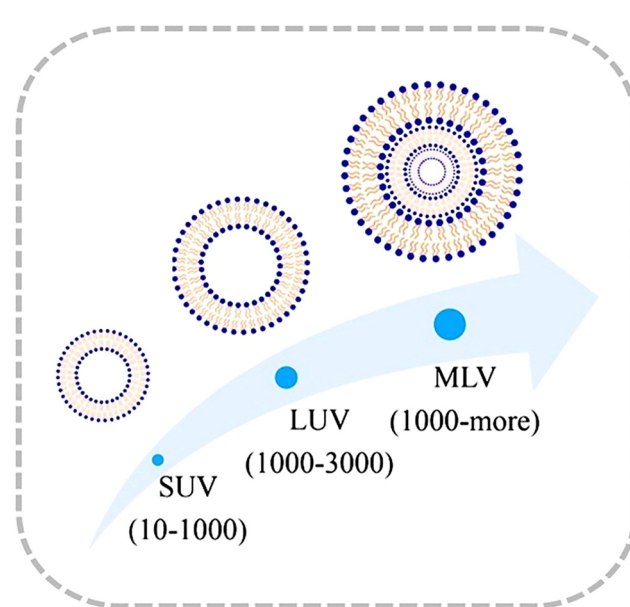


**Fig. 2** Types of niosomes based on their size or number of lamellar layers. Reproduced from ref. 27 with permission from [Society of Pharmaceutical Technocrats], copyright [2021].

soluble medications, and use of fewer lipids.<sup>70</sup> Multiple lipid layers divide the water-filled spaces within MLV. They have a width greater than one micron. MVVs are a type of MLV consisting of tiny vesicles contained within a larger one. MLVs are simpler to produce and maintain compared with other niosomes, and no special techniques are required. They can also store more fat-soluble medications as they possess larger lipid membranes.<sup>71</sup>

Additional niosome varieties include bola surfactant-niosomes, proteasomes, aspasomes, niogelosomes, and vesicle-in-water-and-oil systems (v/w/o). To develop novel niosomal formulations, new surfactants have been created. Nonionic surfactants known as bola-form amphiphiles consist of two identical aza-crown ether groups that function as polar centers and are connected by a prolonged alkyl chain. When they are in close proximity to cholesterol, they can form colloidal systems.<sup>58</sup> Proniosomes are produced through straightforward formulation processes that can be avoided by retaining the composition and known properties of niosomes. They are surfactant-coated carrier granules that can be rehydrated in aqueous dietary materials just before use to produce niosomes. Proniosomal granules have several advantages over their liquid counterparts, including a reduced risk of bacterial contamination and easier administration and transport.<sup>72</sup> Aspasomes are novel nanovesicles composed of one or more ascorbyl palmitate (AP) layers. These bilayer vesicles are advantageous for transdermal drug delivery because they improve percutaneous absorption and stability. Niogelosomes are double-delivery systems (consisting of niosomes and gel) that differ from conventional niosomes in terms of their release characteristics and pharmacokinetics. Researchers are creating niosomal gel for a variety of applications.<sup>35</sup> A vesicle-in-water-in-oil (v/w/o) combination describes the aqueous suspension of niosomes emulsified in another oil component. It is possible to alter the characteristics of the surfactant used to produce the vesicles, the surfactant or combination of surfactants used to immobilize the emulsion, and the composition of the oil component to produce systems with variable limits for drugs or antigens and variable release properties.<sup>73</sup>

### 2.3. Methods of niosome preparation

Various techniques for producing niosomes have been described in the literature. Methods include thin-film hydration, ether injection, microfluidization, transmembrane pH gradient, bubble method, supercritical carbon dioxide fluid, reverse-phase evaporation, and ball milling (Fig. 3). Each technique may generate niosomes with varying size distributions and sizes. The sections that follow provide an overview of several methods for preparing niosomes.

**2.3.1. Thin layer hydration method.** Thin-film hydration, or TFH, is one of the most widely used methods for producing liposomes. In a flask, it is straightforward to combine the membrane-forming compounds with an organic solvent. A layer of the desiccated thin film is produced in the flask following the removal of the organic solvent *via* vacuum evaporation. After disintegrating in an aqueous solution, such as buffer or

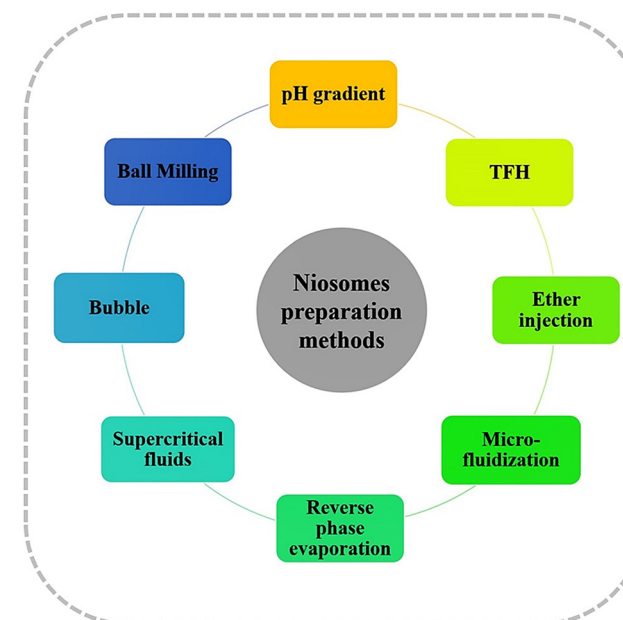


Fig. 3 Preparation methods for niosome formulations using various techniques (such as TFH, ether injection, microfluidization, reverse phase evaporation, supercritical fluids, bubbles, ball milling, and pH gradient). The figure is self-drawn.

water, to rehydrate the desiccated film, the drug is administered. To generate niosomes, it is incubated in a bath of water at a temperature higher than the surfactant's transition point. The TFH technique generates MLVs as a form of niosome. This method is occasionally combined with sonication to generate niosomes with a specific size distribution. This method is frequently used to create niosomes containing drugs such as DOX, insulin, and other derivatives.<sup>74</sup> Waqas *et al.* created a fusidic acid niosomal gel by using the thin layer hydration method. Multiple forms of niosomes of fusidic acid were produced by altering the ratio of cholesterol to surfactant. Niosomes carrying fusidic acid were examined for their morphology using a scanning electron microscope (SEM). SEM micrographs revealed that fusidic acid-loaded niosomes had spherical vesicles with many layers and fluid nuclei.<sup>75</sup>

**2.3.2. Ether injection method (EIM).** EIM was utilized to create a variety of niosomal designs. The EIM is able to prepare SUVs and LUVs spanning in capacity from 50 to 1000 nm. Cholesterol, surfactant(s), and other compounds are dissolved in an organic solvent, such as diethyl ether, in a rotary evaporator vessel. This solution is maintained at a temperature of at least 60 degrees celsius. Under these conditions, a drug-containing water solution is injected slowly, and SUVs or LUVs are produced after the organic solvent evaporates. This method is a viable strategy for the scalability of niosome formulation.<sup>74,76</sup> Using the EI technique, Alkilani *et al.* developed several alendronate sodium (ALS)-loaded niosome formulations. The diameters of the niosomes ranged between  $99.6 \pm 0.9$  and  $464.3 \pm 67.6$  nm. The spherical shape of the niosomes was revealed by transmission electron microscopy (TEM)

imaging, which was used to investigate their morphology.<sup>77</sup> Shewaiter *et al.* developed an EIM-based niosomal formula for acemetacin (ACM). Using TEM images, the morphology of niosomes was investigated. TEM was used to validate the morphological characteristics of the niosomal formulation. TEM images of the optimal niosomal composition revealed the morphology and spherical shape of the niosomes. In addition, TEM analysis revealed that ACM-loaded niosomes were distributed throughout the cell as spherical NPs with distinct boundaries and a porous vesicular shape. The findings had a nearly spherical shape and a polished exterior. Vesicles also dispersed closely at a size of 200 nm, indicating that the particle production factors effectively produced an aggregated and spherical structure.<sup>78</sup>

**2.3.3. Microfluidization method.** This newly discovered method produces unilamellar vesicles that are smaller, more uniform, and have a narrow size distribution. Based on the submerged jet hypothesis, this process involves two fluidized streams traveling at extremely high velocities in the interaction chamber's microchannels. This method forces the surfactant/additives mixture into an ice-filled container using high pressure (100 mL min<sup>-1</sup>). In order to reduce the heat generated by microfluidization, the sample is refrigerated upon exiting the chamber.<sup>79</sup> To achieve the desirable niosomal diameter, the material is reintroduced into the process as often as necessary. This strategy has the benefits of increased homogeneity, reduced size, and unilamellar vesicles.<sup>46</sup> Microfluidic manufacturing was used to create TPT (topotecan)-containing niosomes, according to Selecí and colleagues. By mixing two soluble phases of an aqueous solution with an organic one (lipids dissolved in alcohol) in a microchannel, this technology permits their reproducible fabrication without the need for a subsequent size reduction step. The morphology of the niosomes was determined using TEM imaging and a negative staining technique involving a phosphotungstic acid solution containing 2 percent water. Niosomes appear to have spherical morphologies in the photographs, which may be maintained following specimen processing.<sup>80</sup>

**2.3.4. Transmembrane pH gradient method.** Surfactant and cholesterol are combined and dissolved in chloroform using the transmembrane pH gradient in the round-bottom flask. As a result of the decreased pressure, the organic dissolvent is eradicated. This resulted in the formation of a thin lipid layer on the interior surface of the circular-bottomed flask. This film is hydrated using vortex mixing and a 4 pH citric acid solution. After the completed product has undergone a freeze-thaw cycle, an aqueous pharmaceutical solution is added and agitated using a vortex. This method involves delivering the drug "actively", which captures the pH gradient difference between the basic exterior and acidic interior of the external phase of the ethosomal process. This technique is superior for producing niosomes and encasing fatty substances (such as bud oil and turmeric oil) within niosomes.<sup>81</sup>

Utilizing the transmembrane pH gradient method, Kalaiselvi *et al.* synthesized clove bud oil (CBO)-loaded niosomes with cholesterol and Span 20, 60, and 80 surfactant

types. Niosome aggregation was stopped by the addition of dicetyl phosphate. SEM, FT-IR, and zeta potential examinations were used to analyze the produced niosomes' appearance, functional characteristics, size, and charge. The zeta potential was used to look at the durability of CBO-loaded niosomes and the mean dimension of the particles. The generated CBO-loaded niosomes had a median particle size of 417 nm, and the manufactured niosomes showed excellent stability, according to the data. SEM analysis was used to assess the dimensions and form of the created CBO-loaded niosomes. The results demonstrated the presence of CBO-loaded niosomes in their distinct spherical form. Particle aggregation was absent from the flat surfaces of the CBO-loaded niosomes.<sup>82</sup> Furthermore, Jeno *et al.* produced niosomes encased in Indian plant-based oils by using the transmembrane gradient of pH strategy. Utilizing SEM, FT-IR, zetasizer, and zeta-potential, the obtained niosomes were examined and described. Eucalyptus, neem, and rosemary oils were discovered to contain niosomes with average sizes of 869.64 nm, 693.25 nm, and 912.36 nm, respectively. This suggests more stability. Neem oil was used to create the niosomes, and SEM examination of those niosomes showed similar-sized NPs with a circular structure as well.<sup>83</sup>

**2.3.5. The bubble method.** Using the novel and exclusive "bubble" method, it is possible to create liposomes without an organic solvent. This frothing apparatus has a vessel with a spherical bottom and three stems, and it is submerged in water to regulate the temperature. The thermometer is located in the second neck, water-cooled reflux in the first, and nitrogen supply in the third. Before frothing at 70 °C with nitrogen gas, the surfactant and cholesterol were mixed for 15 seconds at 70 °C in a pH 7.4 buffer.<sup>70</sup>

**2.3.6. Supercritical carbon dioxide fluid method.** Many bilayer vesicles have recently been created using supercritical fluids as an innovative one-step method at low temperatures. A component more than its critical pressure ( $P_c$ ) and critical temperature ( $T_c$ ) is referred to as a supercritical fluid. Supercritical fluids possess the characteristics of density as a liquid and lower viscosity with improved flow characteristics as a gas at the critical point. Due to its high critical pressure ( $P_c = 73.8$  bar) and low critical temperature ( $T_c = 31.1$  °C), carbon dioxide is a gas that is frequently utilized to create supercritical fluid. At the close-to-critical point, CO<sub>2</sub> exhibits significant solvating power characteristics. They can be modified by adjusting the pressure or temperature, precisely as non-polar solvents. Supercritical carbon dioxide (scCO<sub>2</sub>), which is environmentally safe, non-toxic, non-flammable, and economically useful, can be utilized to create bilayer vesicles in place of organic solvents. Water-soluble and thermally unstable substances can be trapped in bilayer vesicles thanks to the low working conditions of scCO<sub>2</sub>. The solvating ability of CO<sub>2</sub> does, nevertheless, have some restrictions for polar compounds and the majority of lipophilic medications when it comes to critical points.<sup>84</sup> Baldino *et al.* produced both empty and theophylline-loaded niosomes using a continual cycle supported by supercritical CO<sub>2</sub>. The excellent outcomes were con-

firmed for up to 30 days in terms of niosome stability and nanometric measurement. While employing a water flow rate of 1 mL min<sup>-1</sup> during the supercritical procedure, a drug encapsulation effectiveness of 85 percent was observed. This series of tests also reliably produced nanometric niosomes, with mean vesicle dimensions between around 160 and 171 nm.<sup>85</sup>

**2.3.7. Reverse phase evaporation method.** The surfactant and cholesterol are dissolved using this approach in a 1:1 ether/chloroform mixture. Then, at 4–5 °C, these two phases are sonicated. The niosome suspension has been diluted in PBS and heated to 60 °C in a water bath for 10 to 15 minutes to produce niosomes. The aforementioned organic phase is removed at 40 °C by introducing a hydration medium and then sonicating the mixture. Niosomes are produced by heating the niosome mixture to 60 °C for 10 minutes, then diluting it with a phosphate-buffered saline solution.<sup>86</sup> Zhang *et al.* manufactured niosomes using a reverse-phase evaporation technique in this situation. Ovalbumin was encapsulated using this method into niosomes composed of Span 80, cholesterol, and stearylamine. The evaluation of the generated niosomes' sizes was conducted using atomic force microscopy (AFM). According to the findings, the effective width of niosomes is around 300 nm. The niosomes have an ellipsoidal form as opposed to being spherical. On the other hand, 200 nm-sized spherical vesicles were shown to exist.<sup>87</sup>

**2.3.8. Ball milling method.** Ball milling (BM) is a top-down approach for constructing nanostructures that use mechanical forces to reduce particulate size. This method, which has recently garnered a great deal of interest, can generate numerous nanomaterials in an efficient, repeatable, and scalable manner. Utilizing a BM strategy, the creation of niosomes for capturing poorly soluble drugs with enhanced drug release patterns is a potential strategy. It provided superior stability, a reduced mean particle size, and a limited dispersion of particle sizes.<sup>88</sup> A superior niosome formulation was created by Temprom *et al.* for the BM method of encapsulating melatonin. The physical properties and stability of the melatonin-loaded and empty niosomes were examined using TEM, dynamic light scattering, and FT-IR analysis. The results showed that the BM method provided excellent stability, a lower mean size, and a narrower size dispersion when niosomes were prepared. Each and every niosomal formulation generated spherical particles with decreased polydispersity index values that were between 250 nm and 600 nm in size. Increasing cholesterol levels were followed by a decrease in the mean size of the niosomes. Additionally, TEM analysis revealed that niosomes are spheres with well-defined walls in both the empty and melatonin-loaded states.<sup>89</sup>

**2.3.9. Other preparation methods.** There are various other methods for preparing niosomes. The freeze and thaw methods are among this approach. These are niosome formulation techniques that have been enhanced over the TFH technique. Liquid nitrogen is used to freeze the TFH-prepared MLV niosome suspension and this is then thawed in a water bath for only a few minutes for a series of repeated cycles.<sup>71</sup> Mokhtar *et al.* developed proniosomal gels or flurbiprofen

solutions. The freeze–thawing/centrifugation procedure for synthesized niosomes outperformed the exhaustive dialysis method in terms of determining the drug entrapment performance.<sup>90</sup> Another method of producing niosomes is the dehydration–rehydration vesicle (DRV) method. Kirby and Gregoriadis provided the first explanation of the DRV approach, which utilized SUVs created using the TFH technique to produce MLVs.<sup>91</sup> In summary, SUVs that had been prepared *via* the TFH approach were extracted using centrifugation. SUVs were then mixed with the drug-containing aqueous phase, and the solution was freeze-dried during the night. Multilamellar DRVs were produced following the rehydration of the final product.<sup>92</sup> The heating method (HM), newly invented by Mozafari for creating nanocarrier structures, is another technique for making niosomes. In a phrase, the medication, cholesterol, and surfactants are introduced to an aqueous phase, like PBS. The aqueous phase is heated and stirred to create the mixture. Next, the solution is given a 3% v/v polyol addition, including glycerol. This approach, which is described as a simple one-step procedure, uses no hazardous, flammable chemical solvents. Table 2 summarizes various methods used so far for preparing niosomal formulations.

### 3. Dual niosomes for cancer therapy

Recent advancements in cancer therapy underscore the crucial role of combination therapies, blending different approaches to enhance effectiveness while reducing the chances of resistance development in cancer cells.<sup>94</sup> It has been noted that recent advancements in chemotherapy have shifted towards utilizing combined dynamic compounds, as they are believed to exhibit enhanced activity compared with a single compound. As a result, the efficacy of treatment may improve, and the side effects on other tissues may be decreased because of combination therapy of an anticancer agent with a herbal bioactive component.<sup>95</sup> The combination strategy of chemosensitizers and chemotherapeutic agents can now be obtained as one nano-transporter. Likewise, the ratiometric load of the drugs had a major impact on their efficiency. Chemosensitizers act on a potency effect and improve the sensitivity of tumor cells to chemotherapy agents.<sup>96</sup> Several efflux pump inhibitors and regulators of MDR proteins like CUR, cyclosporine, and verapamil are now co-administered with chemotherapy drugs to increase their potency.<sup>97</sup> Combination therapy with two or more medicines that promote synergy and multi-functional nano-transporter delivery has proved to be very promising for cancer treatment. Applying two anticancer drugs simultaneously with diverse mechanisms of action can enhance the therapeutic effects, including multiple mechanisms of action.<sup>97</sup> Consequently, it is necessary to formulate such DDS with many anticancer drugs to discover the optimum dual-delivery systems strategy. For instance, DOX efficacy, an anthracycline antibiotic, has been shown to increase if given with antioxidant agents because this medication supposedly induces oxidative stress.<sup>98</sup> To decrease the

**Table 2** Summary of the methods of niosome preparation applied to drug delivery purposes

Composition of niosome	En-capsulated agent	Preparation method	Niosome size (nm)	Key feature	Ref.
Span 60, cholesterol, Cremophor® ELP or Lauroglycol® 90	Methylene blue	TFH	292.4	Production of stable niosomes with optimal lipid content for optimal EE	93
Span 60, TWEEN 60, chloroform, dihexadecyl phosphate chloride, and Carbopol 934	Fusidic acid micropowder	TFH	377.2–725.4	The produced fusidic acid-laden niosomes improved the penetration of fusidic acid <i>via</i> the skin	75
Span 60, Tween 60, Tween 80, cholesterol and diethyl ether	Alendronate sodium	EIM	99.6–464.3	Successfully prepared ALS niosomes for transdermal delivery to offer the prolonged release of ALS and reduce GI negative impacts, and create a replacement production for oral ALS administration	77
Cholesterol, Span 60, diethyl ether	Acemetacin	EIM	315.23	Examination of the utilization of <sup>131</sup> I-ACM niosomes as a potentially effective dual anticancer therapy to combine the chemotherapeutic impacts of ACM and the radiotherapeutic impacts of <sup>131</sup> I in a single treatment cycle	78
Span 60, cholesterol, chloroform and DSPE-PEG (2000) maleimide	Topotecan	Microfluidization	128.5	Improving anti-glioma treatment with tLyp-1-functionalized TPT-loaded niosomes	80
Span 20, 60, and 80, cholesterol, chloroform	Clove bud oil	Transmembrane pH gradient	417	The larvicidal higher performance of the tested mosquito species with the clove bud oil-loaded niosomes and employing these niosomes as possible mosquito repellents	82
Span 60, chloroform, dicetyl phosphate (DCP), and cholesterol	Indian herb oils (neem, eucalyptus, and rosemary)	Transmembrane pH gradient	912.36, 693.25, and 869.64	Niosomes that include neem oil and those made from Indian plant oils may be used instead of commercial mosquito larvicides and have higher rates of larval death	83
Span 80, theophylline powder, Tween 80, cholesterol	Theophylline	Supercritical carbon dioxide fluid	160 and 171	Getting longer theophylline release time of about 5-fold	85
Span 80, cholesterol, stearylamine	Ovalbumin	Reverse phase evaporation	~300 nm	Increasing the niosomal hydrogel platform's antigen delivery in comparison with niosomal elastic gel and taking into account niosomal hydrogel as an excellent transcutaneous antigen delivery carrier	87
Span 60, cholesterol $\geq 92.5\%$ , melatonin $\geq 98\%$ , and phosphate-buffered saline (PBS)	Melatonin	BM	533–266	Exploration of the BM approach as a potentially effective way to create niosomes for the encapsulation of poorly soluble medicines with better drug release profiles	89

TFH; thin-film hydration, EIM: ethanol injection method, BM: ball milling, TPT: topotecan, ACM: acemetacin, ALS: alendronate sodium, MB: methylene blue, EE: encapsulation efficiency.

side effects and increase the availability of chemotherapeutic drugs, encapsulation of these agents with a nanometric vehicle can be the best or most promising approach. In the following sections, we describe the different drugs that are loaded on various niosomal formulations to discover their effects on cancerous cell lines.

### 3.1. Niosomal codelivery of two drugs

DOX is commonly used in combination with tamoxifen (TAM), which is a nonsteroidal selective estrogen receptor modulator applied for the treatment of estrogen receptor-positive breast cancer.<sup>97</sup> On this background, Kulkarni *et al.* entrapped TAM (lipophilic) and DOX (hydrophilic) in a niosome delivery vehicle to attain a combined strategy based on nanomedicines for breast cancer treatment.<sup>57</sup> The combination index (CI) values of free drug and double-charged niosomes results

suggested a significant synergistic impact of niosomes compared with the combination of free drugs. The *in vitro* cytotoxic results show that the double-drug niosomes have improved cytotoxicity for free drugs with significant dose-dependent cell inhibition.<sup>57</sup> This preliminary study showed that the co-loaded niosomes lead to MCF-7 cell inhibition more notably than free drugs or their combination. The IC<sub>50</sub> value of the developed co-loaded niosomes was multiplied by 15 in contrast to the free drugs (Table 3). Optimized niosomes exhibited reasonable EE (>70%) with prolonged drug release patterns of up to 72 hours. A bursting effect was first observed due to the presence of a free drug adsorbed onto the external surface of the nano-carrier. It was followed by a controlled diffusion mechanism from the core caused by the gentle erosion of the bilayer membrane or hydrolysis.<sup>99–101</sup> Additionally, due to cholesterol addition, surfactants are known to become more hydrophobic.

**Table 3** Details of niosomal codelivery of two drugs studies

Compounds	Niosome fabrication method	Surface functionalities	In vitro/in vivo models	IC <sub>50</sub> value (µg mL <sup>-1</sup> )	Cancer type	Key observation	Ref.
1. Tamoxifen 2. Doxorubicin	Box-Behnken design	NA	MCF-7	NA NA	Breast	- Sustained release - Robust drug-excipient compatibility	57
Free doxorubicin + free tamoxifen DDS: doxorubicin + tamoxifen niosome	Thin-layer hydration method	Folic acid	MDA-MB-231	Free doxorubicin + free tamoxifen (0.15 ± 0.3) DDS (0.01 ± 0.3)	Breast	↑Caspase-3	102
1. Letrozole 2. Cyclophosphamide DDS: (NLC) (NLCPFA)	Thin-layer hydration method	Folic acid	SKBR3	48 h: Let (167.47), cyclo (184.91), Let + cyclo (85.76), NLC (47.84), NLCPFA (31.13) 72 h: Let (99.48), cyclo (127.29), Let + cyclo (59.22), NLC (37.53), NLCPFA (23.18) 48 h: Let (147.71), cyclo (109.62), Let + cyclo (67.85), NLC (36.67), NLCPFA (24.92) 72 h: Let (75.77), cyclo (88.33), Let + cyclo (31.01), NLC (28.08), NLCPFA (20.94)	Breast	↑Caspase-3 ↑Cyclin-D ↓Cyclin-E ↓MMP-2	102
1. Epirubicin 2. Cisplatin DDS: (FPNCE)	Thin-layer hydration method	Folic acid	4T1	48 h: CIS (96.36), EPI (135.63), CIS + EPI (87.47), NCE (66.19), FPNCE (50.3)	Breast	↑Bax ↑Caspase3 ↑Caspase9 ↑Mfn1 ↓Bcl2 ↓Drp1 ↓MMP-2 ↓MMP-9 Reduction in: invasion, mitosis index, pleomorphism in BALB/c mice Severe hyperchromicity observation in BALB/c mice	103
1. Farnesol 2. Gingerol DDS: N-Far + Gin	Box-Behnken design	NA	MCF7	48 h: niosome (1263.45), Gin (986.9), Far (192.46), Gin + Far (131.99), N-Gin + Far (25.56)	Breast	↑P21 ↑Bax ↑CASP-3 ↑CASP-9 ↑BCL2 ↓JHER2 ↓CDK4 ↓CCND1 ↓CCNE - High antioxidant potency - Improved cellular uptake efficiency	104
1. Rifampicin 2. Ceftriaxone 1. Cisplatin 2. Gemcitabine	Ecological probe sonication method Heating method (optimized by D-optimal mixture design)	NA NA	SKBR3 MRC5 A549	72 h: niosome (1166.31), Gin (583.65), Far (125.267), Gin + Far (95.27), N-Gin + Far (19.563) 48 h: niosome (2230.06), Gin (986.495), Far (233.628), Gin + Far (165.09), N-Gin + Far (44.01) 72 h: niosome (1097.27), Gin (958.434), Far (183.005), Gin + Far (134.227), N-Gin + Far (26.58) NA NA 72 h: niosome (>500), CIS (<1.56), Gem (<1.56), Gem + Cis (<1.56), NGC (280) 72 h: niosome (>500), CIS (66), Gem (<1.56), Gem + Cis (<1.56), NGC (46)	NA NA NA NA	- Improved drug release and entrapment - Faster <i>in vitro</i> drug release rates - Improved drug release and entrapment	105 106

DDS: drug delivery system, NLC: niosomes loaded with (letrozole + cyclophosphamide), NLCPFA: surface-functionalized with a folic-acid-targeting moiety, NCE: cisplatin and epirubicin-loaded niosome, FPNCE: FA-PEGylated niosomal cisplatin and epirubicin, N-Far + Gin: farnesol-gingerol-loaded niosome, NGC: niosome-loaded (cisplatin + gemcitabine).

As a result, compact niosomes are formed, which support subsequent drug release. When the length of the alkyl chain is enhanced, the drug release rate declines.<sup>100</sup> On the other hand, drug uptake and *in vitro* cytotoxicity results have shown that the optimized DDS has shown more effective tumor inhibition and considerable localization than any other single therapeutic agent. These findings suggest a deep therapeutic application of dual-loaded (TAM + DOX) niosomes with modified cholesterol formulations (without any surface functionalities) for combined breast cancer treatment.<sup>57</sup>

In another study for the breast cancer therapy field, Sahrayi and co-workers have developed nanoscale niosome-based transporters as targeted delivery systems.<sup>102</sup> The developed platform is composed of dual-loaded niosomes with letrozole (Let) and cyclophosphamide (Cyclo) (NLC), and folic acid (FA) functionalized on the surface (NLCPFA) and can activate apoptosis, reduce Bcl-2 expression, and increase Bax expression by targeting the PTEN/AKT/P53 signaling pathway.<sup>107</sup> Niosome NPs contain an equal amount of both drugs, and formulation optimization features have been investigated using various surfactant-cholesterol molar proportions of 1:1 and 2:1 and lipid-drug molar proportions of 10:1 and 20:1, that affected the EE.<sup>108</sup> EE values of samples improved by 2–3% for each drug at the greater surfactant:cholesterol and lipid:drug molar proportions. It was suggested that the thicker bilayer could have greater encapsulation potential for hydrophobic drugs,<sup>109–111</sup> and also the presence of FA may increase the EE. Additionally, the mean size of the modified NPs was lower than that of the NLC. According to the CI, both drugs have considerable synergistic effects against MDA-MB-231 and SKBR3, but the NLCPFA group had a higher cytotoxic effect on the cancer cells, which was probably caused by the interaction of FA-coated niosomes with folate receptors on breast cancer cells, leading to the active transportation of niosomes within cells.<sup>112,113</sup> Based on IC<sub>50</sub> values (Table 3), a synergistic effect was evident when both drugs were administered, which had a far more toxic effect than each single drug for both cell lines. Furthermore the cytotoxicity effect was enhanced by the addition of FA to the functionalized niosome, perhaps due to folate receptor-mediated endocytosis, which increased the cellular uptake of drugs. FA plays a vital role in cell growth, differentiation, repair, and host defence, as demonstrated in Fig. 4A. NLCPFA significantly enhanced total apoptosis in both cancerous cells, and cell cycle analysis in Fig. 4B and C showed a strong synergic effect and niosomal co-loaded delivery of both drugs causing a shift toward the sub-G1 phase in each cancerous cell. NLCPFA produced a greater change in the effectiveness of the drugs.<sup>102</sup> This study showed that, along with the synergistic effect of dual-drug niosomes, coated FA can inhibit the activity of breast cancer cells by promoting the apoptosis of both MDA-MB-231 and SKBR3 cells.

In another study on the effects of FA-coated niosomes and the codelivery of cisplatin (CIS) and epirubicin (EPI), two chemotherapeutic drugs for breast cancer treatment, Moammeri and his colleagues designed an FA-PEGylated niosome (FPNCE) to produce a functionalized DDS based on co-loaded

niosomes to increase endocytosis and finally injected it into BALB/c mice (Fig. 5A).<sup>103</sup> The formulation was pH-responsive because hypoxia in cancerous cells and tumor tissue usually causes a decrease in pH value. CIS is an effective hydrophilic drug for human cancer treatment because it can cause apoptosis and DNA damage in cancerous cells.<sup>114</sup> EPI, which has reduced cardiotoxicity and is a semisynthetic analog of DOX, is a hydrophobic functional drug used to treat breast cancer. EPI can inhibit topoisomerase II and plays a vital role in cancer therapy by inhibiting DNA replication and lipid peroxidation.<sup>115,116</sup> The *in vitro* release profile results indicated that the release of drugs from NCE and FPNCE samples at a pH of 5.4 is remarkably higher than the release at pH 7.4, indicating that the designed DDSs are pH-responsive. This can be attributed to the electrostatic interaction between the positively charged drugs and PEG chains, and the ionization state at physiological pH. Additionally, the obtained data indicated that the delayed drug release of FA-PEGylation caused greater drug aggregation in target cells and that an acidic pH ruptured the niosome structure, which led to enhanced toxicity.<sup>117</sup> The increase in vesicle size and polydispersity index (PDI), as well as the reduction rate in EE for the FPNCE, was lower than that for the NCE throughout the shelf life. Therefore, the data show that FA-PEGylation can also stabilize the DDS formulation because the polymer-coated niosomes decreased systematic phagocytosis.<sup>54</sup> Based on the *in vivo* results shown in Fig. 5B and C, the number of tumors decreased significantly in BALB/c mouse in FPNCE-treated tumors and the anticancer efficacy of FPNCE also significantly mitigated tumor size and enhanced body weight mass, as FA inhibited the expression of anti-apoptotic genes such as Bcl2. Following FPNCE treatment, invasion, mitosis, and nuclear polymorphism were reduced. Local drug delivery, cytotoxicity efficacy, and apoptotic body creation showed that nano-niosome FA-PEGylated was an appropriate nano-based delivery system for dual drug delivery.<sup>103</sup> The addition of FA to the surface of niosomes has been shown to induce apoptosis in breast cancerous cell lines, as indicated by the results of the last two studies. The amount of FA receptors on the surface of normal cells is less than that on cancerous cells, so it can be hypothesized that the surface modification of niosomes can play a key role in the cellular uptake of the drugs and targeted delivery. Table 3 summarizes the details of the studies on dual delivery niosomal systems.

Recent research has aimed to formulate and characterize an advanced system of pH-responsive drug administration based on farnesol-gingerol-loaded (N-Far/Gin) niosomes (without surface modification) as a new method for breast cancer treatment.<sup>104</sup> N-Far/Gin showed outstanding biocompatibility with the control human foreskin fibroblast (HFF) cells, indicating remarkable cytotoxicity against SKBR3 and MCF7 cell lines. Similar to other loaded niosomal DDSs, endocytosis is the penetration method of entrapped drugs into cancerous cells, and internalization is facilitated by the hydrophobic surface and smaller size of the niosome. N-Far/Gin causes apoptosis in SKBR3 and MCF7 cells through the syner-

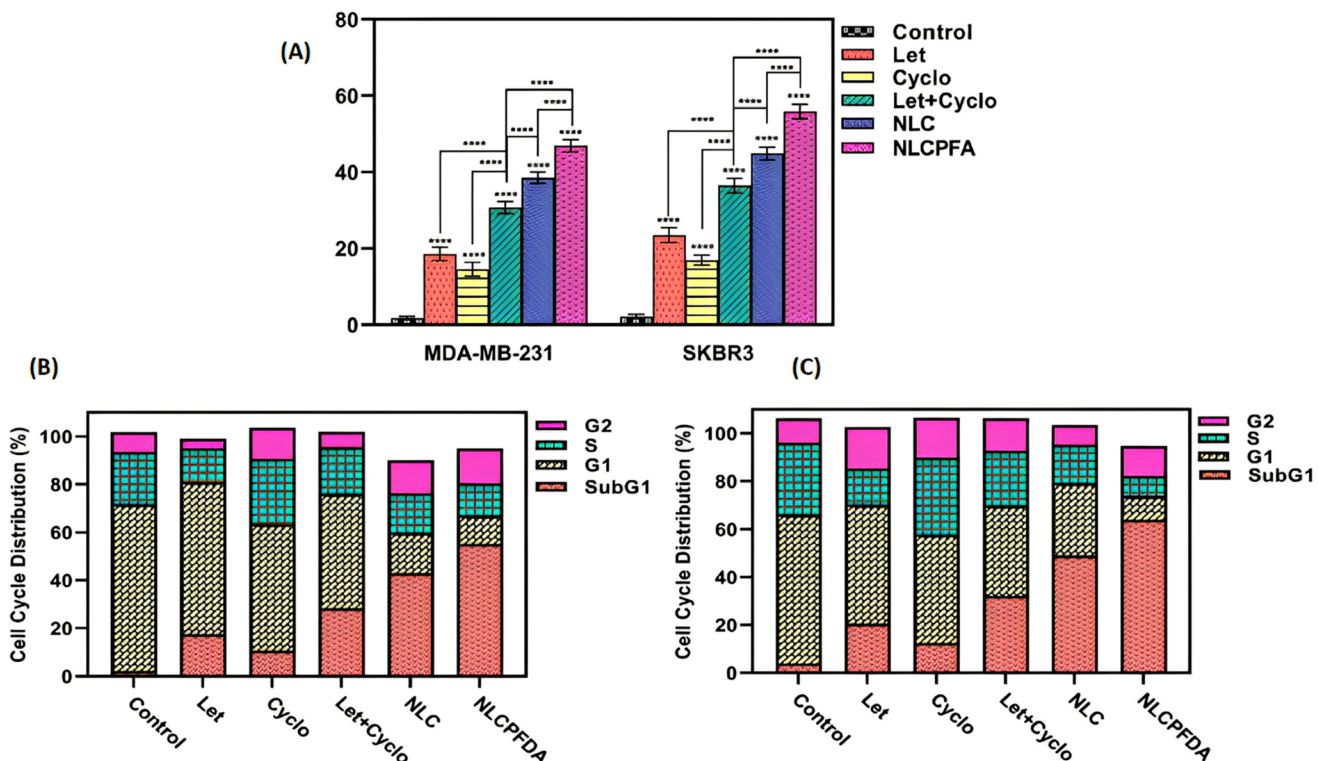


**Fig. 4** (A) Analysis of the total apoptosis of cancer cell lines (MDA-MB-231 and SKBR3) after treatment by free drugs and various niosomal structures. NLCPFA significantly increases total apoptosis in cancerous cells treated in increments of 21.9% for MDA-MB-231 and 24.5% for SKBR3, as opposed to NLC formulations. The cell cycle analysis graphs of (B) MDA-MB-231 and (C) SKBR3 cancer cells after treatment with a variety of niosomal and free drug formulations. Reproduced from ref. 102 with permission from [MDPI], copyright [2021].

gistic effect of the drugs, as reported by apoptosis tests, by increasing the expression of anti-apoptotic genes (Table 3).<sup>104</sup>

To produce another niosomal formulation for co-loading treatment using the ecological probe sonication approach, Khan *et al.*<sup>105</sup> utilized rifampicin (Rif), a biopharmaceutics classification system (BCS) class II drug with low water solubility, and ceftriaxone sodium (Cfx), a BCS class III drug with poor permeability.<sup>118,119</sup> Owing to the undesired free-form characteristics of these drugs, they have been chosen as appropriate candidates for DDS encapsulation. To increase niosome function as nano-carriers, a combination of non-ionic surfactants from Pluronic L121 and Span 60 was considered for the niosome structure. By adding two or more non-ionic amphiphiles, more stable, monodisperse, and smaller niosomes with improved drug release profiles and a high EE% can be achieved.<sup>120</sup> Cellular uptake can be improved by smaller niosomes, which results in greater anticancer effectiveness.

A combination of CIS and gemcitabine (GEM) for lung cancer therapy *via* aerosolization against normal (MRC5) and cancerous (A549) lung cell lines was studied by Mohamad Saimi *et al.*<sup>106</sup> The results from this study showed that the optimized formulation of niosomes with a low dose of CIS and Gem (NGC), small particle size, and three-month stability can be applied for cancer therapy. CIS and Gem have shown good interaction in a dual delivery experiment for lung cancer cell treatments, with the potential to be more effective towards

cancerous cell lines and the ability to decrease side effects in comparison with systemic drug release due to their low toxicity in neutral blood conditions.<sup>121</sup> The EE% results demonstrated that CIS entrapment efficiency was greater than that of Gem. This was caused by the polarity of the drugs, where CIS was less polarized than Gem. As a result, CIS can easily cross the lipid bilayer membrane and Gem is expected to pass passively through the lipid bilayer membrane and become entrapped in the aqueous core.<sup>106</sup> The ability to inhale the niosome formulation is a patient-friendly method that has the potential for further lung cancer treatment studies. Such research is based on the low surface tension of the formulations and high electrostatic charge, which can result in a high aerosol output.

### 3.2. Niosomal codelivery of a drug and natural plant-based bioactive compounds

Plants with significant chemical diversity have been widely studied for centuries for their anticancer potential. For instance, CUR, a hydrophobic polyphenol bioactive compound, is produced by the rhizome of *Curcuma longa*. CUR has a wide range of pharmacological potential, including anti-inflammatory, antioxidant, and anti-tumor effects, and is presently administered in the early phase of a clinical trial as a potential chemo-preventive component. Due to its immensely low instability, aqueous solubility, high metabolic rate, and poor bioavailability, the pharmacological application of CUR

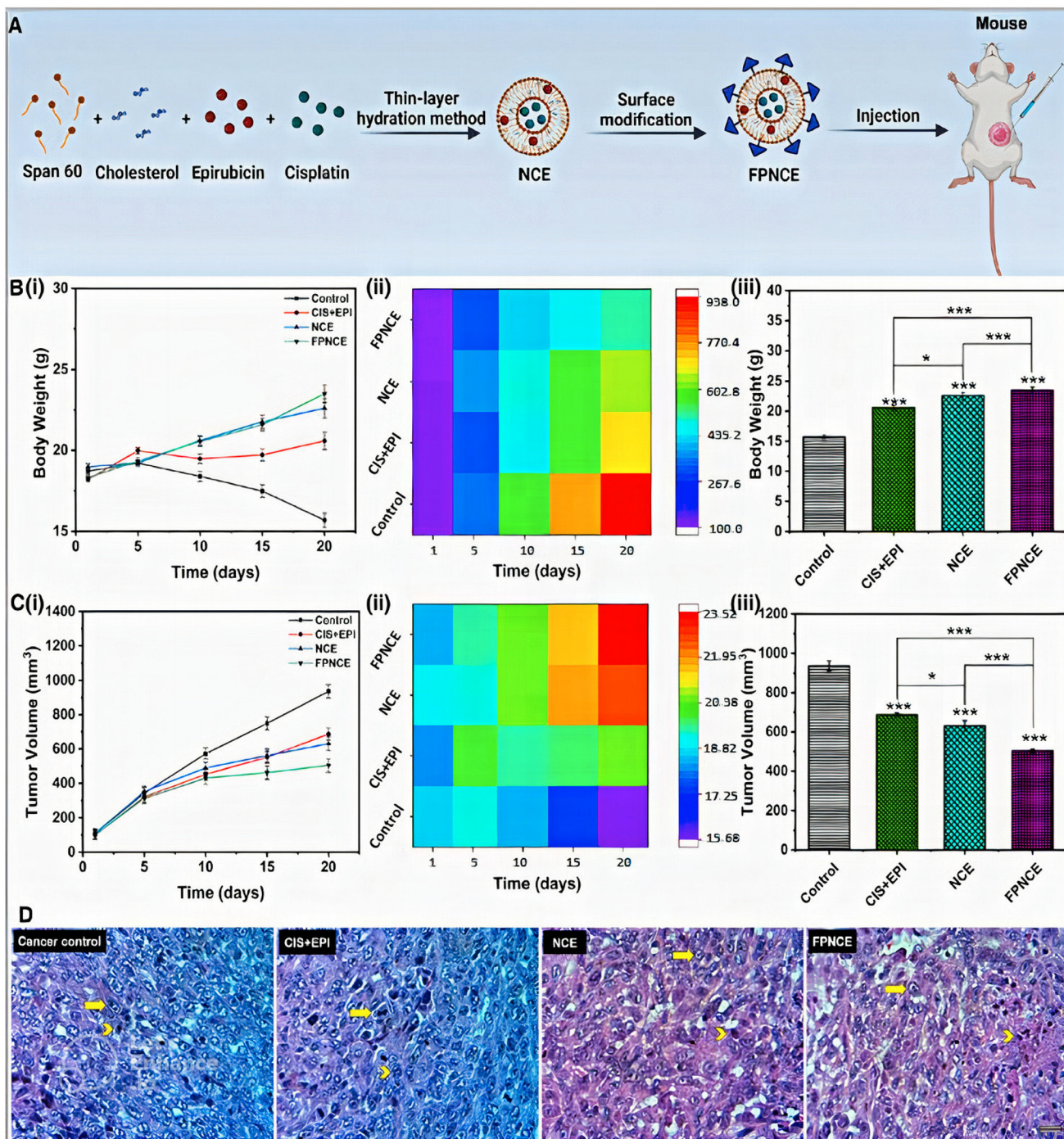


**Fig. 5** (A) Illustration of a diagram showing the simultaneous injection of CIS and EPI into a BALB/c mouse. (B) Mass of the animal body during the course of therapy compared with days (i), and the mouse body weight heat map (ii). The weight of the mouse after 20 days of treatment (iii). (C) The heat mapping of the volume of the tumor (ii) and the observation of tumor volume during therapy *versus* time (i). The volume of the tumor on day 20 of treatment (iii). (D) Malignant breast tumors are examined under a microscope; the malignant control, CIS + EPI, NCE, and FPNCE are stained with H&E. Nuclear polymorphism is shown by arrowheads, and cancer tissue by arrows (magnification 400 $\times$ ; scale bar equals 50  $\mu\text{m}$ ). Reproduced from ref. 103 with permission from [American Chemical Society], copyright [2022].

has been hindered.<sup>122–124</sup> CUR has also been utilized against cancers by blocking the nuclear factor kappa B (NF- $\kappa$ B) signaling pathway and downregulating the overexpression of Bcl-2 and P-glycoprotein.<sup>125</sup> The co-encapsulation of CUR along with

other agents in niosomes has been widely investigated, such as human glioblastoma (U87)<sup>126</sup> and tamoxifen against MCF-7,<sup>127,128</sup> and DOX-LipoNiosome loaded against Saos-2, KG-1, and MG-63 cell lines,<sup>54</sup> which are listed in Table 4. In

**Table 4** Summary of niosomal codelivery of a drug and natural plant-based bioactive compound investigations

Compounds	Niosome fabrication method	Surface functionalities	In vitro/in vivo models	IC <sub>50</sub> value (µg mL <sup>-1</sup> )	Cancer type	Key observation	Ref.
1. DOX 2. PTX	Probe sonication method	NA	MCF-7 PC3-MM2	NA	Breast Prostate	- Sustained drug release - Improved antiproliferative effects in time- and dose-dependent manner	129
1. PTX 2. OXP	Thin film hydration	NA	HT-29	PTX (19.98) OXP (23.56)	Colorectal	- Extended drug release - Increase the cellular uptake of both drugs - Increased cytotoxic and apoptosis activity - Increased cellular interaction - Enhanced cytotoxicity	130
1. CUR 2. DOX DDS: PEGNIO/DOX + CUR/t-Lyp-1	Thin film hydration	PEG Modified with tumor-homing and penetrating peptide (t-Lyp-1) DSPE-mPEG	U87	48 h: DOX + CUR (0.96) PEGNIO/DOX + CUR (0.9) PEGNIO/DOX + CUR/t-Lyp-1 (0.76) NA	Glioblastoma	- Increased cellular interaction	126
1. CUR 2. DOX DDS: (Lipo)Niosomal	Thin film and pH gradient technique	Naos-2 MG-63 KG-1 MCF-7		CUR (63.12) TMX (41.98) CUR + TMX (36.12) Nano (CUR + TMX) (20.68)	Osteosarcoma	- Improved drug loading capacity, anti-proliferative	54
1. CUR 2. TMX CUR + TMX DDS: nano (CUR + TMX)	Thin-layer hydration	NA			Breast	↑Bax ↑p53 ↓Bcl2 - Controlled release at physiological pH - Burst release at acidic pH	127 and 128
1. Gem 2. Tocotrienols	Handjani-Vila and film hydration methods	NA	AsPC-1 SW 1990 Panc 10.05 BxPC-3	NA	Pancreatic	- Improved the efficacy of drug combination with a 9-fold increase in cytotoxicity	131
1. CUR 2. Let	Thin-layer hydration	FA PEG	MCF-7 MDA-MB-231	NA	Breast	↓Cyclin-D ↓Cyclin-E ↓Bcl2 ↑Bax ↑Caspase3 ↑Caspase9 ↑p53	47
1. Artemisinin (Art) 2. CUR DDS: Cur-Art-loaded Niosomes	NA	NA	SW480	DDS (10.39)	Colorectal	- pH-dependent release behavior - Appropriate drug release	132
1. Let	Thin-layer hydration	FA	MDA-MB-231	48 h: Let + AA (422.67), Let + niosome (255.5), AA + niosome (791.76)	Breast	↓Cyclin-D	133
2. Ascorbic acid (AA) DDS: folate-PEGylated Let-AA-niosome	PEG		SKBR3 MCF-10A	48 h: Let + AA (298.32), Let (457.5), AA (819.4), Let-AA-niosome (75)		↓MMP-2 ↓MMP-9 ↑Caspase3 ↑Caspase9	

DDS: drug delivery system, PEG: polyethylene glycol, FA: folic acid.

the DOX–CUR LipoNiosome pH-responsive study, different cell lines were used in a delivery system to demonstrate the anti-proliferative performance of these drugs (Fig. 6A–E). The enhanced release profile was influenced by various conditions such as temperature, pH, and the structure of the LipoNiosome membrane (Fig. 6F and G). A cytotoxicity assay confirmed the pH-responsive nature of the designed formulation. The anticancer action of DOX was effectively enhanced by concentrating CUR in cancerous cells using a carrier. Both the drugs were delivered sustainably through the prepared formulations. Due to the low pH value of the lysosome, which causes the carrier membrane to loosen, drug release in cells is enhanced.

The other herbal product, paclitaxel (PTX), an essential antineoplastic drug, is extracted from *Taxus brevifolia* bark. PTX shows effective chemotherapeutic and cytotoxic potential against many types of cancer. However, the overall therapeutic effects of PTX are restricted due to poor water solubility and low therapeutic index.<sup>134,135</sup> To overcome these limitations and improve the therapeutic potency of cancer therapies, Alemi *et al.*<sup>95</sup> developed a DDS to co-administer PTX and CUR in PEGylated niosomal formulations for increased effectiveness in MCF-7 cells. The system remarkably decreased MCF-7 cell growth to a greater extent than the free PTX/CUR combination (Table 4). The combination of PTX with niosomes and another anticancer drug, oxaliplatin (OXP), has been studied by El-Far *et al.*<sup>130</sup> to encapsulate drugs in an optimized

niosome and develop their therapy results against colorectal cancer. Delivering dual drug-loaded niosomes altered the release profile compared with that of their free drugs, as they revealed a widened drug release, causing a reduction in their toxicity. The encapsulation of OXP and PTX into the niosome significantly increased their cytotoxicity and apoptosis activity by up to two- or threefold compared with the free drugs. Adding  $\alpha$ -tocopheryl polyethylene glycol 1000 succinate (TPGS) to the niosome preparation can affect the apoptotic activity of drug-loaded niosomes through different mechanisms, such as the participation of TPGS in the inhibition and destruction of the mitochondrial respiratory complex<sup>136</sup> and the induction of DNA damage or oxidation of proteins, enzymes, and lipids, which lead to cell destruction.<sup>137</sup> In other words, TPGS could increase bioavailability and reverse MDR.<sup>136,138</sup> PTX was also co-encapsulated with DOX and delivered *via* niosomes to study the DDS in MCF-7 and PC3-MM2 cancer cell lines. The niosomes revealed a high EE and a synergistic effect due to the presence of both drugs, which can overcome MDR.<sup>129</sup> Let is co-administrated with a supplementary and natural drug ascorbic acid (AA) by Bourbour and her colleagues<sup>133</sup> to decrease the side effects of Let, and both are loaded on a similar folate-PEGylated niosome<sup>47</sup> (*i.e.*, folate-PEGylated Let-AA-niosomes). It was found that the remarkable anti-cancer activity of the niosomal DDS was due to the dual-loading of Let and AA. In addition, investigations have shown that PEG has no cytotoxic potential. Thus, the increase in cytotoxicity

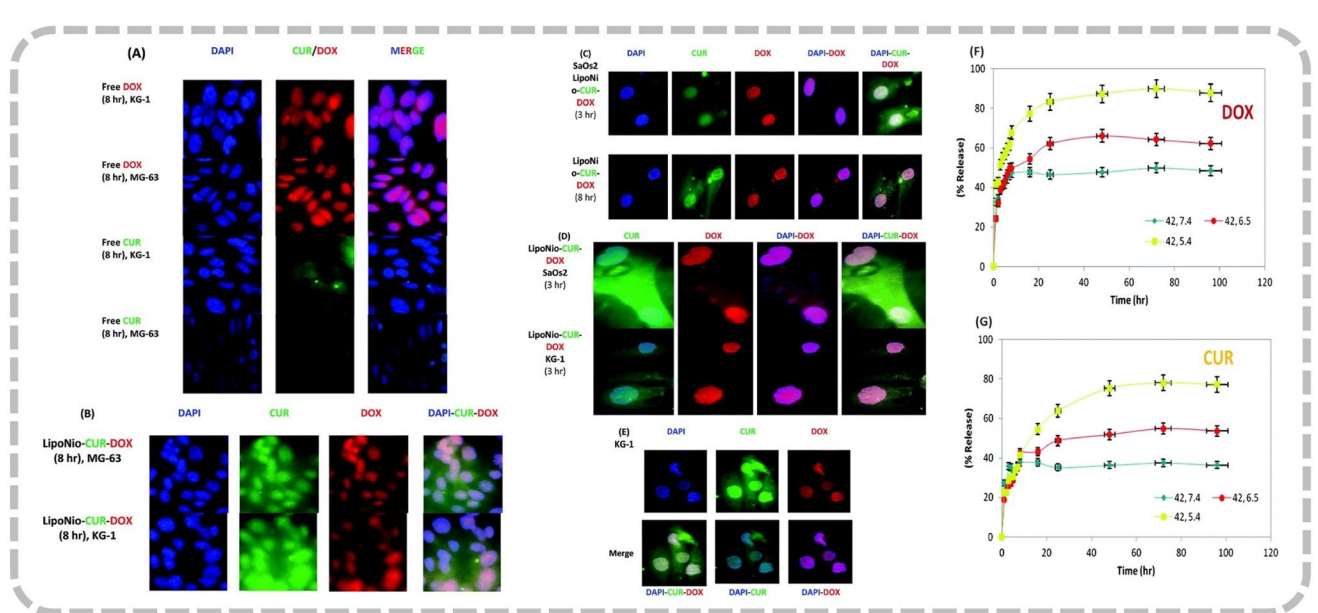


**Fig. 6** Cellular uptake images of MG-63, KG-1, and SaOs2 osteosarcoma cancerous cell lines, treated with free DOX and CUR and drugs entrapped into LipoNio carriers. For staining the nuclei, DAPI was applied. DOX and CUR have red and green fluorescence, respectively. (A) The comparison between the cellular uptake of free drugs after 8 h-treatment in the KG-1 and MG-63 cell lines; (B) cellular uptake results of MG-63 and KG-1 cells treated with LipoNio-DOX–CUR; (C) cellular uptake of SaOs2 cells treated with LipoNio-DOX–CUR for 3 and 8 hours; (D) cellular uptake of SaOs2 and KG-1 cells treated with LipoNio-DOX–CUR for 3 hours; (E) typical features on merging. Treated cells with entrapped drugs have shown more violet and turquoise blue color intensity than free drug-treated cells. Entrapped drugs could penetrate cells by endocytosis, while the diffusion mechanism transported free drug molecules. (F) and (G) The drug release profiles in PBS at pH 7.4, 6.5, 5.4, and a temperature of 42 °C. Reproduced from ref. 54 with permission from [Royal Society of Chemistry], copyright [2017].

activities in cancerous cells by the FA-Let-AA-niosome is due to the release of both loaded drugs inside the cells (good cellular uptake) and not to the components of the niosomal formulation itself.<sup>139,140</sup> In Fig. 7, the invasion (A) and (D), migration (B) and (E), and scratch (C) results are demonstrated. The FA-LA-niosome and FA-niosome effectively inhibited migration in both cancerous cells, which could potentially lead to FA cytotoxicity by upregulating Bax, PTEN, and p53, as previously mentioned in FA-surface-functionalized studies.

FA-functionalized niosomes have been optimized and co-loaded with CUR and Let as a promising DDS for breast cancer cell therapy.<sup>47</sup> Both drugs are anticipated to exist chiefly in the niosome lipid bilayer, depending on their hydrophobic nature. These results revealed that the niosomal formulation utilizing a lipid/drug proportion of 10 was considerably smaller than the same formulations with a lipid/drug proportion of 20. A greater amount of lipids in the niosomal formulation could form larger NPs and a thicker lipid bilayer.<sup>141</sup> In addition, the mean size of niosomes was significantly increased, which was confirmed by drug encapsulation.<sup>47</sup> Owing to the presence of FA in the formulation, the niosomal formulation had significant inhibitory effects on both the MDA-MB-231 and MCF-7 cell lines, which is consistent with the results of Sahrayi *et al.*<sup>102</sup> The details of recent studies on the codelivery of drugs and herbal-based molecules are listed in Table 4.

### 3.3. Niosomal codelivery of drug/bioactive compounds and nucleic acids

Discovering and regulating the genes responsible for cancer pathology is of continuous interest in discovering new approaches to cancer therapy.<sup>142,143</sup> An increasing number of investigations have revealed that RNA interference (RNAi) is a favorable gene manipulation method with therapeutic potency when administered alone or in combination with other treatments, and is a tumor-selective gene silencing approach.<sup>144,145</sup> In addition, the therapeutic effectiveness of anticancer drug molecules can be remarkably enhanced by the additive or synergistic effects induced by siRNA and combination methods.<sup>56</sup> Oncogenes play a vital role in various stages of cell growth in cancerous cell lines and may be considered targets of these types of RNA.<sup>146</sup> siRNA is a well-known RNAi specifically designed to silence the gene expressions implicated in drug resistance<sup>34</sup> and chemotherapy inactivity. It has also been extensively studied for combination therapies.<sup>53,147</sup> Because of their size and negative charge, siRNAs cannot cross the cell membrane;<sup>148</sup> consequently, there are problems in the systemic *in vivo* delivery of bare siRNA to targeted sites because of limited blood stability, poor intracellular uptake, and nonspecific immune stimulation, which restrict the siRNAs' therapeutic development.<sup>148</sup>

In this regard, to enhance the inherent therapeutic efficacy of siRNAs, it has been demonstrated that nano-DDS improves the stability of siRNA, increases selectivity to the target, prevents premature degradation, and enables fast *in vivo* clearance of siRNAs. One of the most interesting delivery systems in the

study of niosomes and siRNAs is the possibility of loading various drug molecules into niosomes to increase the efficacy of cancer treatments. To prove this, Hemati and her colleagues developed cationic PEGylated niosomes that could co-encapsulate siRNA and DOX against cell division cycle 20 (CDC20).<sup>51,53</sup> At the cell-cycle checkpoint (G2/M), CDC20 is a regulatory protein that interacts with an anaphase-promoting complex/cyclosome (APC/C), initiating anaphase. In cancerous cells, CDC20 upregulation has been shown to result in increased cell proliferation, tumor initiation, and cancer development;<sup>149</sup> hence, CDC20 siRNA can suppress cell growth and target the G2/M phase. The first study was conducted in three cancerous cell lines: human gastric cancer (AGS), human adenocarcinoma prostate cancer (PC3), and MCF7. The drug release profile showed sustained release, and cellular uptake data *via* endocytosis revealed that the number of cancerous cells treated with Nio-DOX was higher than that in the group treated with the free drug. Additionally, it has a key function in delivering the combination of DOX and siRNA through cell membranes, compared with free drugs that penetrate through a diffusion mechanism. The results indicated that the dual encapsulation of drugs and siRNA in cationic PEGylated niosomes showed an enhanced anti-cancer potential against the death of tumor cells.<sup>51</sup>

The second study by the same team focused on gastric cancer treatment with CDC20 siRNA and anticancer drug molecules to target cell cycle proteins, as previously mentioned.<sup>53</sup> Quercetin (QC) is an herbal drug and chemo-sensitizer. It can also prevent tumor proliferation by activating the intrinsic path of apoptosis and blocking the phase S during the progression of the cellular cycle.<sup>150,151</sup> DOX/QC/siRNA was loaded into a different niosomal formulation. The various molar ratios of dioleoyl-3-trimethylammonium propane (DOTAP) were evaluated to optimize the niosomes for advancing the loaded siRNA. The DOTAP addition leads to a reduction in the vesicle size, which was discovered by Campbell *et al.*,<sup>152</sup> and PDI, which is related to the reciprocal repulsion force existing among the particles with the same charge in a suspension system.<sup>153–155</sup> Also, the cellular uptake results indicated that the DOTAP addition improved the DOX/QC/siRNA transfection potential.<sup>153,154</sup> This resulted in cationic lipids that improved the optimized niosome transfection potential. Apoptosis analysis revealed that there was a remarkable increase in the cell death rate when DOX and siRNA were co-delivered due to a synergistic effect on apoptosis induction. These results demonstrated that the synergistic antitumor activities and controlled release of siRNA/anticancer drug-encapsulated niosomes could downregulate the expression of CDC20 with high efficiency, resulting in a synergistic therapeutic reaction, ultimately causing gastric cancer elimination.<sup>53</sup>

Many studies have shown that the addition of DOTAP improves the niosome characteristics and the release of loaded drugs and nucleotide acids. The DOTAP presence in gene and bioactive compound niosomal formulations to boost transfection efficacy and stability has been followed by Abtahi and her

## MDA-MB-231 Cell Line

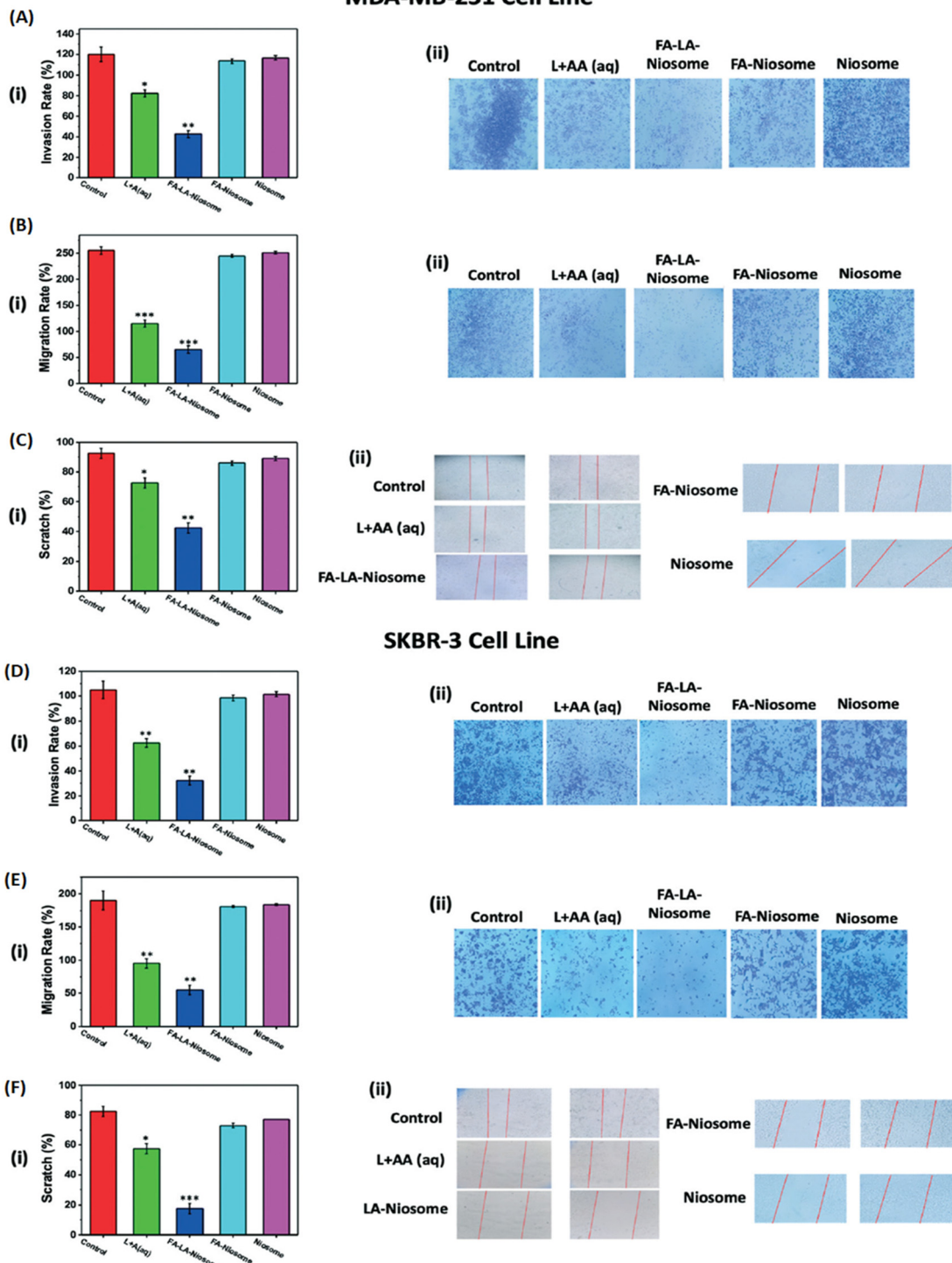


**Fig. 7** (A) and (D) Invasion, (B) and (E) migration, and (C) and (F) scratch results (i) microscope images (ii) for the MDA-MB-231 cells and SKBR3 cells (control) after treatment with an aqueous solution of (Let + AA), FA-Let-AA-niosome, FA functionalized bare niosomes (FA-niosome), and bare niosome. Magnification: 10×. Bar chart showing the average number of cells that invaded through the pores during the Matrigel experiment. The results are shown concerning values measured in cells with no treatment (blank group) and depict average values  $\pm$  SD from at least three independent experiments. The inhibition in the SKBR3 cells was higher than in the MBR-MB-231 cell line. Reproduced from ref. 133 with permission from [Royal Society of Chemistry], copyright [2022].

colleagues.<sup>156</sup> MicroRNA-34, a member of the p53 network, is one of the tumor-inhibiting microRNAs. A potential target of miR-34a in breast cancer is regulating the type of silent mating information 2 homolog 1 (SIRT1) oncogene.<sup>157</sup> Down-regulation of miR-34a in various tumors has been proved. Many studies have revealed the potential of miR-34a in cancer therapy by targeting nano-DDS. Based on the results (Fig. 8), after two months of storage, the vesicle size, PDI, and percentage of EE of the optimized niosomal structure demonstrated no remarkable changes in comparison with the synthesized samples, which verifies the physical stability of niosome-CUR for up to two months (Fig. 8A). To investigate the impact of extended storage on miR-34a leakage from the outer surface of the niosomes, samples were stored at 4 °C for up to four months. Fig. 8B demonstrates that even after four months, the structures were stable with the lowest leakage. The reason for this stability is the presence of DOTAP in the niosomal formulations. In a previous study,<sup>106</sup> the stability of niosomes was measured for three months, but in the formulation, sodium dodecyl sulfate (SDS) was used instead of DOTAP. To stabilize the niosomes, the particle size is reduced, and the negatively charged zeta potential is increased, which leads to electrostatic repulsion between the niosome particles and prevents aggregation. Furthermore, the graph in Fig. 8C illustrates that DOTAP is not cytotoxic. Consequently, the incorporation of DOTAP into niosomes has both physical and physiological benefits. According to the tumor growth graph (*in vivo*), the niosome codelivery system could increase the tumor inhibition activity and present a synergistic therapeutic impact higher than that

of co-delivering or free structures of both miR-34a and CUR (Fig. 8D and E). The results from the curve (Fig. 8F) indicated that the mice treated with a co-delivery system (loaded with miR-34a and CUR) showed a slight change in body weight. The data showed that niosomal codelivery did not enhance the toxicity compared with niosome-miR-34a and niosome-CUR.<sup>156</sup>

Similarly, the impact of DOTAP on the niosomal delivery system, transfection efficiency in MCF-7 cells, vesicle size, and PDI were investigated in a recent study by Abtahi and co-workers.<sup>158</sup> miR-34a was loaded alone on novel PEGylated niosomes in different formulations. Following the addition of 5–15% DOTAP, the zeta potential increased, and there was a reduction in the PDI and average size. Also, the findings indicated that the presence of PEG on the niosome surface along with DOTAP resulted in increased stability and reduced average diameter. The *in vivo* study revealed that the body weight of niosomal miR-34a-treated mice decreased slightly after three weeks. These findings are consistent with those of niosome-miR-34a-CUR-delivery in their previous study.<sup>156</sup>

### 3.4. Niosomal codelivery of two gene agents

As discussed earlier, RNAi therapy in the field of gene treatment has become a special and promising technique that involves gene expression modulation and silencing of genes at the transcriptional level. Co-loaded niosomes have been utilized to enhance the transfection efficiency and control restrictions in gene treatment. Newly designed delivery strategies for miRNAs to tumor sites to eliminate them have attracted attention and have been applied in both *in vitro* and *in vivo*

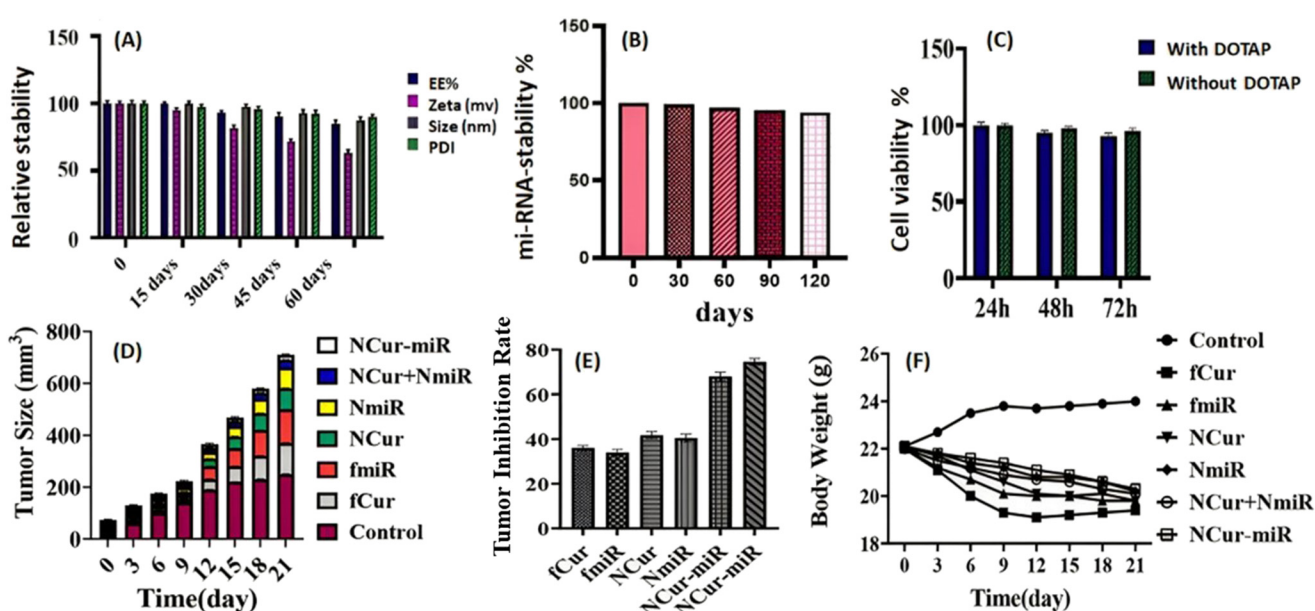


**Fig. 8** (A) Physical stability of niosome-CUR after 15, 30, 45, and 60 days, (B) time-dependent stability of miR-34a loaded niosomes, (C) cytotoxic effect of DOTAP addition to the niosome structure, (D) impact of different structures on mouse weight, measured every 3 days, (E) effect of different structures on the tumor size (cm<sup>3</sup>) of the mouse models of breast cancer (cases treated with the structures for 21 days. A digital vernier caliper measured the tumor volumes. In the 2nd and 3rd weeks after therapy tumor volumes were remarkably less than that of the control groups), (F) mouse body weight graph (data were presented as the mean  $\pm$  SD, and  $P < 0.05$  was considered a significant statistical difference). Reproduced from ref. 156 with permission from [Elsevier], copyright [2022].

investigations.<sup>159–161</sup> Tumor suppressor micro-RNAs, including miR-15a and miR-16-1, can regulate a group of oncogenes.<sup>162</sup> However, they may be downregulated or eliminated in many types of cancer, such as chronic lymphocytic leukemia (CLL),<sup>163</sup> gastric cancer,<sup>164</sup> and breast cancer.<sup>165</sup> miR-15a and miR16-1 have the potential to target different genes, including MCL-1, WNT3A, CCND1, and Bcl-2.<sup>166,167</sup> Therefore, they can inhibit cell growth, induce apoptosis, and target malignant cell proliferation by silencing anti-apoptotic genes. The extensive diversity of cancerous cells, including PC3 cells, uses various scenarios to break apoptosis. As the simultaneous use of miR-16-1 and miR-15a revealed the strong activity of the onco-suppressor, the synergistic application of both miRNAs may significantly impact the suppression of cancerous cell growth. In this regard, the co-delivery of these two miRNAs could represent a promising treatment approach for prostate cancer in its progressive stages, which was studied by Ghaffari *et al.*<sup>52</sup> Consistent with other studies,<sup>156,158</sup> the presence of DOTAP in the niosomal formulation led to the enhancement of positively charged particles. Additionally, PDI and vesicle size were linearly reduced with an increase in DOTAP molar levels. The cytotoxicity assay data showed that miR-15a/miR-16-1 co-loaded on niosomes considerably decreased the survival of PC3 cells, indicating that therapy with free miRNAs and the niosome-loaded system led to the inhibition of PC3 cell growth depending on the dosage. Also, fluorescent microscopic analysis (Fig. 9) showed that the niosome-labeled DIL was delivered successfully to the cancer cells. Fluorescent imaging findings suggested that niosomes with minimal cytotoxicity can increase cellular uptake as well as electrostatic interactions with the cell membrane. According to transfection efficiency data, miRNAs significantly decreased the expression of Bcl-2 after 48 hours at the first level of gene expression (transcription) compared with the single niosome-treated cells. These results are consistent with those of Bonci *et al.*, who investigated the expression of Bcl-2 in the same cancer cell lines.<sup>168</sup> Additionally, cells transfected with the co-loaded niosome and miR15a-/miR16-1 delivery system showed a marked decrease in Bcl-2 expression compared with those transfected with miR15a-niosome and miR16-1-niosomes.<sup>52</sup>

Another study on the dual-gene-loaded niosome field was conducted by Gharbavi and his co-workers.<sup>169</sup> NANOG, a homeobox protein, is an important transcription factor and has an essential involvement in stem cell mitosis. Furthermore, it has been discovered that it is a key player in maintaining the carcinogenic properties of various cancer types and glioblastomas.<sup>170,171</sup> Additionally, by upregulating the multidrug resistance mutation (MDR1), NANOG can increase chemoresistance, which makes it an optimistic target for cancer treatment.<sup>172</sup> The decoy oligodeoxynucleotides (decoy ODNs), a class of nucleic acid-based drugs, are short double-stranded DNA molecules. This therapeutic method can be a safe, efficient, and promising approach for eliminating cancerous cells.<sup>173</sup> Previously, BSA-coated niosomes (NISM@B) were synthesized through a thin-layer hydration approach by the same researchers, and the obtained data revealed that

NISM@B has efficient therapeutic agent binding potency, high uptake efficiency, and low cytotoxicity.<sup>174</sup> In this regard, NANOG decoy ODNs were loaded into NISM@B to form NISM@B-decoy ODN complexes (NISM@B-DEC) to study the capacity of the delivery system for the cancerous cell line U87. A steady DDS was successfully prepared with a regular spherical form and narrow size distribution with acceptable zeta-potential results and biocompatibility. The ODNs released from the DDS demonstrated a controlled and pH-responsive profile as the best model for explaining the ODN release pattern. Finally, NISM@ B-DEC efficiently reduced tumor formation, was taken up by the U87 cell line, and markedly inhibited cell growth.<sup>169</sup> According to a small number of studies, this codelivery system may be promising for cancer treatment. However, due to the complicated method and gene loading, the obtained studies are insufficient and warrant further investigation.

### 3.5. Niogelosomes

Niogelosomes, produced from polymeric gels and niosomes, are dual-loaded delivery systems, and their pharmacokinetics and release characteristics vary from those of free niosomes.<sup>175</sup> The presence of polymeric gels such as PEG<sup>47,103</sup> and hyaluronic acid<sup>176</sup> could increase their bioavailability and loading efficiency, preventing drug leakage from the niosome and therapeutic applications for different treatments. In addition, other polymers, such as chitosan, which has mucoadhesive potential, can offer multiple benefits to delivery systems by enabling a targeted delivery and guiding niosomes toward MUC1-overexpressing tumor cells.<sup>19,177</sup> Polymeric gels can protect niosomes against fluctuations in external tonicity and prevent uncontrollable and early niosome bursts and drug release. However, in the delivery site, polymeric gels may reduce drug release ability. This restriction can be controlled by utilizing agents that respond to pH reduction or temperature enhancement in the cancerous sites. This leads to the preparation of smart stealth niosomes, which can release most loaded drugs at their delivered cancerous site instead of other healthy tissues.<sup>178</sup> Double packaging by applying gel as the outer layer stabilizes the niosomes' surface, modulating the cargo release over time.<sup>179</sup> To observe the advantage of polymeric gels in niosomal delivery, Wiranowska *et al.* studied the estimation of a chitosan-based DDS by applying a new *in vitro* model to compare the potential of targeting carcinoma cells to IMMC3 and IOSE-121 epithelial normal cells.<sup>179</sup> This system contains fluorescence-labeled PTX encapsulated in niosomes incorporated into a thermosensitive cross-linked chitosan hydrogel and constructed for the controlled, prolonged, and localized delivery of loaded drugs. Outside of the treated epithelial origin carcinoma cells (OV2008), the fluorescence intensity was measured at various diffused distances at three different sites, inhibiting the difference in fluorescence intensity averages in those sites with the highest fluorescence intensity around the cell surface showing a concentration gradient, most probably guided by the high affinity of chitosan to the MUC1 receptors.<sup>179</sup>

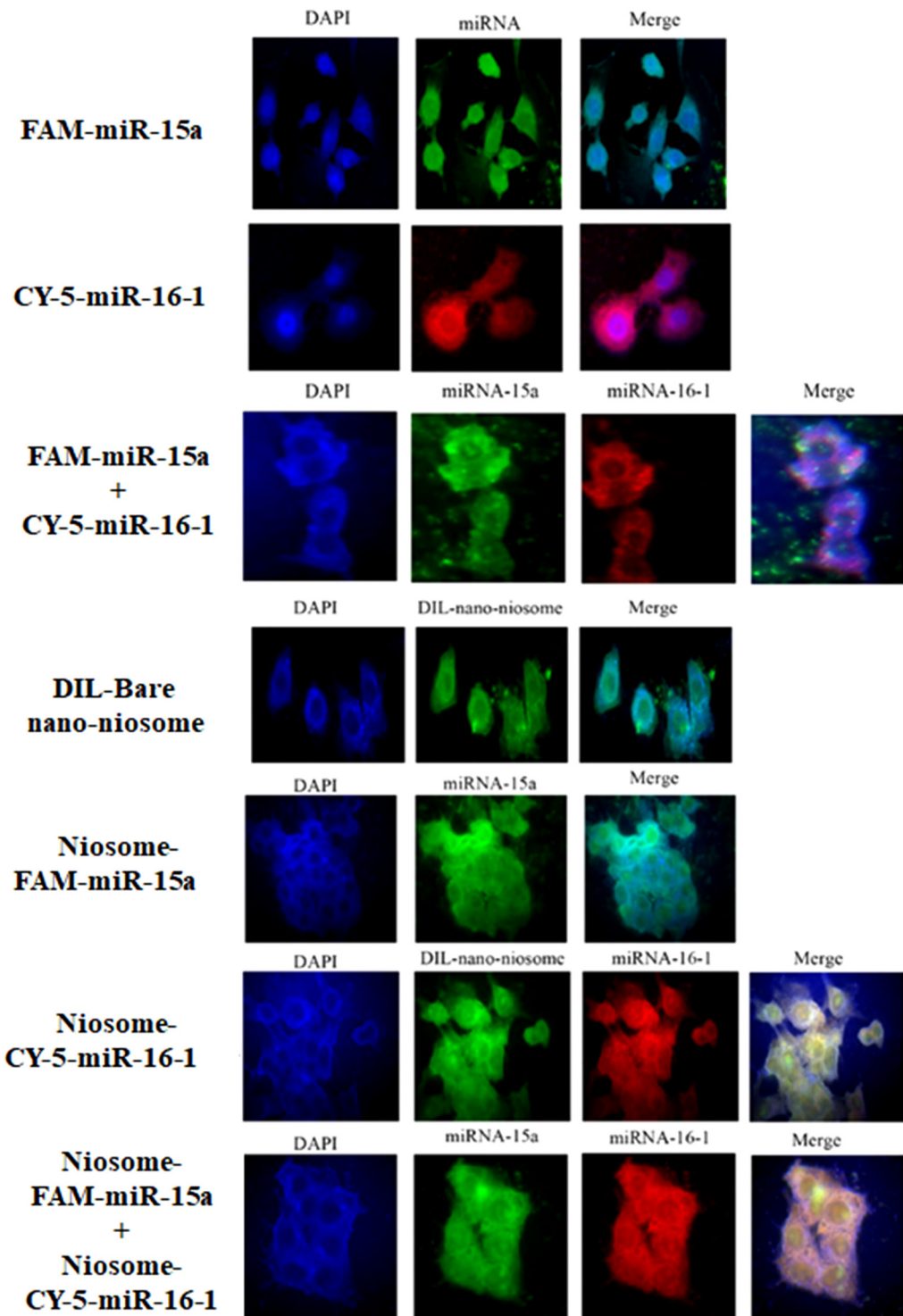


**Fig. 9** Fluorescent microscopic images of the uptake of free miRNAs, bare niosomes, and co-loaded DDS 3 hours after transfection. miRNAs co-loaded niosomes showed a greater cellular uptake rate and higher turquoise-blue and purple intensity compared with free miRNA-treated cells. The average fluorescence intensity and the greatest percentage of cellular uptake belong to miR15a-/miR16-1 loaded niosomes. DAPI was used to stain cell nuclei (blue), and 4% paraformaldehyde was utilized to fix transfected cells (960 magnification). Fluorescence intensities were calculated by ImageJ and plotted as mean fluorescence intensity. \* $p < 0.05$ . Reproduced from ref. 52 with permission from [Springer], copyright [2021].

Recently, a new study aimed to design a novel smart nano-DDS with anticancer and antibacterial properties that can be used for lung cancer treatment.<sup>180</sup> This DDS is prepared from

a niosomal encapsulating CUR as an anticancer agent and is embedded in a chitosan gel structure containing Rose Bengal (RB) as a dye with photodynamic antibacterial capability. The

fabricated system exhibited a high EE% for both drugs and temperature- and pH-sensitive release profiles. The antibacterial activity of carriers was evaluated using the colony formation technique and was applied against a Gram-negative (*E. coli*) and a Gram-positive (*S. aureus*) bacterium. RB inhibited the antibacterial effects against both bacterial strains, but prepared DDS only showed bacterial inhibition and antibacterial activity against *E. coli*. The designed DDS might be acceptable for lung cancer treatment because Gram-negative bacteria could promote cancer development alongside the synergistic effect of the two drugs and other good properties.<sup>180</sup> Another study presented an advanced dual-loaded delivery system for intravesical application prepared from CUR/gentamicin sulfate (GS)-loaded niosomes embedded in thermo-responsive *in situ* gels (CUR/GS-co-loaded niosomes).<sup>55</sup> The main portion of the chosen gel was Poloxamer 407, with adequate mucoadhesive and reversible gelation (depending on temperature) properties. The thermosensitive behavior of the *in situ* gel DDSs has been investigated by oscillation tests in time sweep mode. The test is applied to discover the required time for transition from a liquid state (room temperature 25 °C) to gel form (body temperature 37 °C) after administration in the body. This transition initiated within 20 seconds, whereas the gel state appeared after 35 seconds. This is a typical gel-dominated behavior by the elastic portion and shows a sufficient transition time in the body. The results depicted that adding niosomes to *in situ* gels did not change the physical stability; only a small enhancement in size (less than 10%) was observed due to polymer deposition on the niosomal surface. The results showed that the CUR/GS compound in the niosomal-embedded gel was more conserved at the end of the study compared with those in niosomes without gel.<sup>55</sup>

To evaluate chitosan hydrogel, in another experiment, chitosan-coated niosome (ChN) was utilized to increase the bioavailability of both boswellic acid (BA) and CUR drugs.<sup>181</sup> Many studies have suggested different medicinal effects of BA, which include anti-carcinogen, anti-inflammatory, anti-arthritis, and memory impairment features. However, there are disadvantages, including low solubility and low bioavailability.<sup>182</sup> The characteristic analysis of samples showed that at low levels of chitosan, the average particle size of ChN was reduced compared with bare niosomes (BN). It has been suggested that ultrasound processing after the adhesion of chitosan to the outer layer of niosomes caused this reduction. Moreover, increasing the concentration of chitosan enhanced the average vesicle size. The creation of a thicker chitosan coat and chitosan bridges among particulates caused an increase in particle size at higher chitosan levels.<sup>181</sup> In advanced technologies, the prototyping method and nanotechnology have opened novel cancer cell treatment areas.<sup>183</sup> The emergence of the 3D-printing method has produced numerous updated possibilities for polymer hydrogel-based drug administration approaches, particularly for cancer therapy.<sup>184,185</sup> 3D-printing prepares controllable and organized scaffolds with excessive precision, which might give rise to the prolonged and mediated release of various agents and molecules, such as proteins and different

types of drugs in a possible and acceptable procedure.<sup>186</sup> Hosseini *et al.* recently presented a novel DDS based on 3D-printed gelatin-alginate biodegradable scaffolds incorporating paclitaxel-loaded niosomes (Nio-PTX@GT-AL) for breast cancer therapy.<sup>183</sup> Due to the presence of alginate, the printed scaffolds are pH-sensitive DDSs for cancer treatment. According to the mechanical properties (tensile and compressive states) of Nio@GT-AL and Nio-PTX@GT-AL, the existence of drug-containing niosomes leads to a slight enhancement in modulus and strength in both the compressive and tensile states, which may lead to prolonged stability. The activity of caspase-3, caspase-8, and caspase-9 has been demonstrated in Fig. 10. Treated cells with free-PTX, Nio-PTX, Nio@GT-AL, and Nio-PTX@GT-AL markedly enhanced the activity of the three caspases. However, niosome-containing samples, mostly Nio-PTX@GT-AL, have improved the activity of caspase considerably more than free-PTX.<sup>183</sup>

Various parameters must be considered when designing an efficient dual delivery niosome system. The use of material combinations, such as surfactants, is necessary to translate the niosome formulation method. The characteristics of these materials include size, morphology, stability, PDI, EE, zeta potential, and even cytotoxicity, and gene induction, such as DOTAP, as previously mentioned. The therapeutic impact of these materials is both dual and effective. Also, drug properties, such as hydrophobic and hydrophilic properties, as well as their molecular size, play a crucial role in achieving a high EE%. Surface modification is another solution to optimize niosome characteristics. (i) Using polymers with different molecular weights and characteristics has a considerable effect on niosome properties. The stability of niosomes is facilitated by PEGylation, a biocompatible biomaterial. Niogelsomes, such as chitosan, can also cause sustained drug release or aid in targeted delivery. (ii) Various agents, such as FA (vitamin B9), may have dual impacts in optimizing DDS by increasing EE and biological effects by attaching cancer cell receptors to increase endocytosis. Therefore, there are different methodologies to prepare targeted DDSs along with the synergistic effects of dual drugs. To examine the efficacy and therapeutic dose of dual drugs, it is necessary to conduct more *in vivo* experiments because the pharmacokinetic and pharmacodynamic effects are measurable in a body condition.

## 4. Dual-niosomes for other therapeutic purposes

### 4.1. Cutaneous drug delivery

Incorporating antioxidants into sunscreens is a logical step to capture free radicals generated by UV light that penetrates the skin's outer layers. As a result, the co-delivery of these antioxidants and UV filters has become a challenge. Niosomes, which increase permeation and facilitate direct vesicle fusion with the stratum corneum, can enhance the permeation of encapsulated drugs. Arslan Azizoglu *et al.* proposed a combination

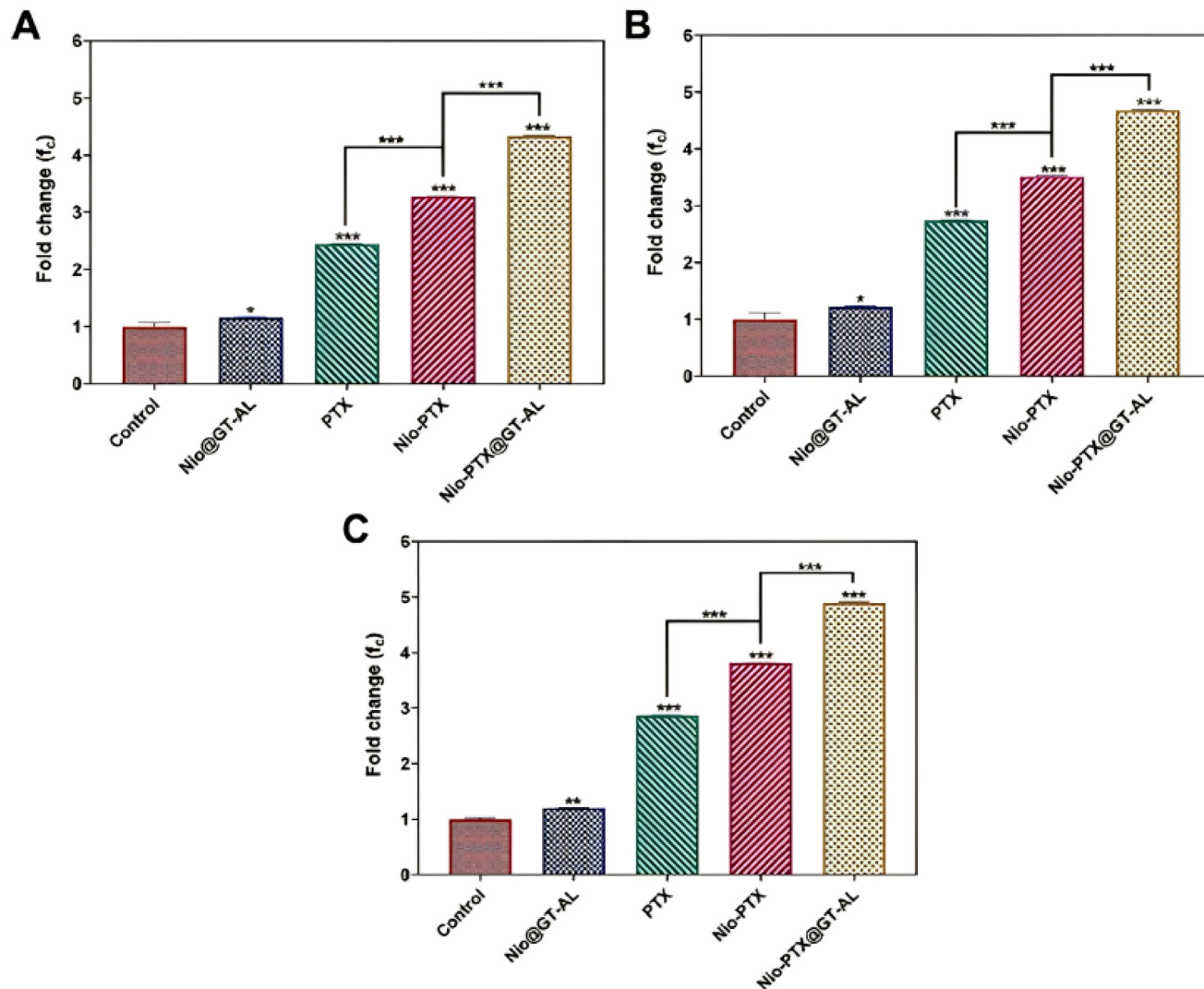


**Fig. 10** The comparison of activity of caspase-3, caspase-8, and caspase-9 in niosome-containing scaffold therapies and free-drug (PTX). An enhancement in the activity and expression of three caspases can be observed as an index of the capability of the cancer therapy system. (A) Caspase-3; (B) caspase-8; and (C) caspase-9. Nio-PTX@GT-AL has distinctly shown the most increase in the activity of all three types of caspase, leading to a 5-fold improvement in comparison with the control group ( $P$ -value =  $P$ , \* $P$  < 0.05, \*\* $P$  < 0.01, \*\*\* $P$  < 0.001). Reproduced from ref. 183 with permission from [Elsevier], copyright [2023].

therapy where octyl methoxycinnamate, a chemical UV filter, accumulates on the skin's upper layers, and melatonin, an antioxidant, penetrates deeper into the epidermis layers to exhibit its antioxidant, photoprotective, and anticarcinogenic activities.<sup>187</sup> They developed a new dual-niosomal formulation by combining melatonin-encapsulated elastic niosomes and a Pickering emulsion of octyl methoxycinnamate stabilized by silica particles. The elastic niosomes were uniformly sized in the nanometer range, while the Pickering emulsions contained octyl methoxycinnamate in micrometer-sized droplets. *Ex vivo* permeation studies showed that 7.40% of octyl methoxycinnamate and 58% of melatonin permeated through rat abdominal skin, with 27.6% of octyl methoxycinnamate and 37% of melatonin accumulating in the skin after 24 hours. The safety of the proposed dual formulation was assessed using a real-time

cell analyzer, and it was found to have no negative impact on cell proliferation or viability. The antioxidant activity of the formulation was studied using 1,1-Diphenyl-2-picrylhydrazyl (DPPH) free radical scavenging experiments, which confirmed its high antioxidant activity. These results suggest that the dual-niosomal formulation has potential applications in delivering multiple therapeutic agents with high efficacy and safety.

Psoriasis is an immune-mediated skin disorder. Methotrexate is often the first line of treatment, but its low solubility and systemic toxicity can limit its use. Yang *et al.* addressed this issue by using ceramide-based niosomes (cerosomes) to dual load methotrexate and nicotinamide (NIC) to reduce toxicity and increase treatment efficiency.<sup>188</sup> The combination of methotrexate and nicotinamide can synergistically

influence psoriasis treatment. Nicotinamide's hydrotropic and anti-inflammatory properties can enhance the solubility and efficacy of methotrexate and decrease the production of pro-inflammatory factors. In their study, cerosomes were used to deliver methotrexate and nicotinamide to deeper skin layers. This reduced the skin thickness and the expression of pro-inflammatory cytokines in psoriatic skin. *In vitro* and *in vivo* permeation studies showed that the cerosomes significantly increased methotrexate and nicotinamide permeation and retention in the skin. Methotrexate/nicotinamide cerosomes demonstrated potent anti-proliferative effects on HaCaT cells irritated by lipopolysaccharide by arresting the cell cycle at the S phase and inducing apoptosis. In imiquimod (IMQ)-induced psoriatic mouse model, using methotrexate/nicotinamide niosomes improved skin lesions compared with the oral administration of methotrexate. This approach also reduced the spleen index and epidermal thickness while down-regulating the expression levels of pro-inflammatory cytokine mRNA (Fig. 11).

Nevertheless, the application of dual-niosomes, a specific category of drug delivery system, faces significant obstacles, specifically in the context of cutaneous drug delivery. A significant concern pertains to the efficacy of drug delivery systems, as certain medications may accumulate prior to permeating their intended site or fail to reach the epidermis. Moreover, the assertions regarding the effectiveness of dual-niosomes have yet to undergo replication or peer review by other scientists, which presents a substantial barrier to their acceptability. Additionally, the potential systemic toxicity of particular medications, such as methotrexate, may impose restrictions on their usage. While there have been suggestions to enhance treatment effectiveness and mitigate toxicity through the use of ceramide-based niosomes, the extent of their potential adverse effects and long-term ramifications has yet to be investigated.

## 5. Treatment of infections

Bacterial resistance to multiple antibiotics is one of the global public health concerns which causes infectious diseases and also leads to the failure of many antibacterial treatments. Hence, developing novel procedures to treat bacterial infections has received much attention.

### 5.1. Tuberculosis

*Mycobacterium tuberculosis* (MT) causes a highly dangerous disease due to factors such as its lengthy diagnosis process, ease of transmission, therapeutic adherence, resistance, and prevalence. The prevention of tuberculosis has become a significant concern for global control. Kulkarni *et al.* developed dual niosomes for the co-delivery of D-cycloserine and ethionamide, creating a novel formulation to combat drug-resistant MT.<sup>101</sup> They used the Box-Behnken experimental design to determine the optimal formulation variables. The optimized formulation showed over 70% entrapment efficiencies, an

ideal particle size of 137.4 nm, and sustained release for up to 3 days. It also demonstrated good stability over six months. Antimicrobial investigations further confirmed the synergistic effect of the D-cycloserine/ethionamide niosome compared with the free combination of drugs. This suggests that the proposed formulation could be an effective therapeutic approach for tuberculosis treatment.

In another study, Khan and colleagues examined the encapsulation of ceftriaxone sodium and rifampicin in niosomes using the eco-friendly probe sonication procedure for tuberculosis treatment.<sup>105</sup> The optimized formulations showed very high drug entrapment efficiencies for ceftriaxone sodium and rifampicin, with values exceeding 96%. Additionally, some drug release studies revealed that the niosomal formulations had faster *in vitro* ceftriaxone sodium and rifampicin release rates than pure ceftriaxone sodium and pure rifampicin.

### 5.2. *Pseudomonas aeruginosa* and *Staphylococcus aureus*

*Pseudomonas aeruginosa* (PA) is an opportunistic pathogen that can cause infections primarily in individuals with compromised immune systems. This bacterium forms biofilms, which can lead to prolonged medical treatments and even fatalities among patients. Biofilms act as barriers, making it difficult for antibiotics to penetrate and leading to a persistent immune response and chronic infections. High doses of drugs are often required to effectively treat PA infections associated with biofilms. In response to this, various researchers have proposed the use of combination therapy, where two or more drugs are used, to combat the antibiotic resistance displayed by biofilm-forming bacteria. Mahdian *et al.* used niosomes as a self-assembled dual drug delivery carrier to load tobramycin and bismuth-ethanedithiol for the treatment of PA. This approach aimed to inhibit the formation of biofilm and the production of *N*-acyl homoserine lactone by PA.<sup>24</sup> The study specifically investigated the effects of several combinations of bismuth-ethanedithiol, tobramycin, and niosomal formulations on the growth of *Agrobacterium tumefaciens* strain. The results showed that the combination of niosomal tobramycin and niosomal tobramycin incorporated with bismuth-ethanedithiol was the most effective in inhibiting the growth of different PA strains. This significantly decreased the minimum inhibitory concentration of tobramycin, leading to a reduction in the rate of biofilm formation and inhibiting the production of the *N*-acyl homoserine lactone molecule. Therefore, encapsulating tobramycin and bismuth-ethanedithiol in niosomes can increase antibacterial activity and reduce antibiotic resistance.

Sohrabi *et al.* prepared and characterized chitosan gel-embedded moxifloxacin-loaded niosomes as a potential drug carrier for topical antimicrobial delivery.<sup>189</sup> The designed moxifloxacin niosomal gel hybrid system showed sustainable release behaviors. The antibacterial efficacy of various formulations was studied by evaluating the minimal concentrations for inhibition, minimal concentrations for a bactericidal effect, and an assay of agar diffusion by PA and *Staphylococcus aureus* (SA). The results of antimicrobial experiments exhibited that niosomal formulation played a remarkable role in

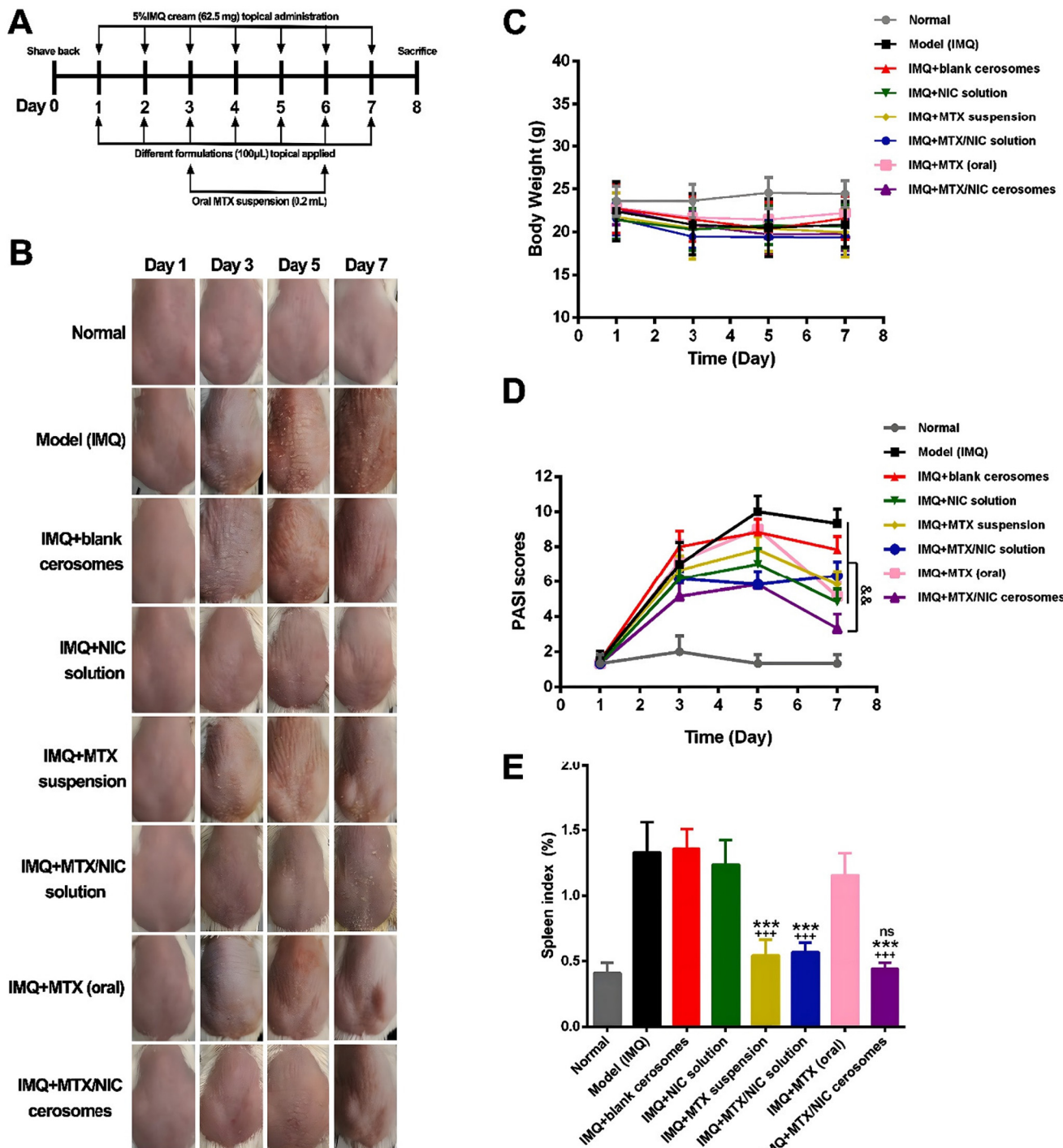


**Fig. 11** (A) A schematic illustration of the procedure for the animal model and treatment of IMQ-induced psoriasis. (B) Photographs of the dorsal epidermis of rodents treated with various formulations for 1, 3, 5, and 7 days. (C) Throughout the investigation, each group's physical weight changed. (D) PASI of epidermis on days 1, 3, 5, and 7 ( $\&P = 0.01$ ). (E) The scores are added together and reported as cumulative scores. Spleen index following seven days of therapy. No statistically significant difference between the normal and model groups; \*\*\* $P < 0.001$  between the MTX (oral) and model groups; \*\*\* $P < 0.001$  among the normal and histological groups. Reproduced from ref. 188 with permission from [Elsevier], copyright [2021].

increased anti-PA efficacy. Chitosan gel-embedded moxifloxacin niosomes could guarantee an extended local retention and better effectiveness due to high drug loading, prolonged drug

release, and bioadhesive behaviors. Therefore, the hybrid system has potential as an efficient novel platform for the controlled delivery of antimicrobial agents.

Targhi and co-workers have investigated the synergistic effect of silver/copper NPs and CUR against *PA* and *SA*.<sup>190</sup> The niosomal formulations and their hydrogel counterparts were evaluated to study their antibacterial activity against *SA* and *PA* using disk diffusion, and assays for the minimum concentration for an inhibitory effect, and minimum concentration for a bactericidal effect. Furthermore, to study the anti-biofilm effect of the samples, anti-biofilm assay and biofilm-associated gene expression by real-time PCR have been used. The niosomal formulations exhibited high drug entrapment efficiencies with a prolonged release of drug patterns over 72 hours. A crystal violet assay was used to study the anti-biofilm performance of the materials. The results of the crystal violet assay displayed that CUR-AgNP-loaded niosomes, CUR-CuNP-loaded niosomes, CUR-AgNP-loaded niosomal hydrogel, and CUR-CuNP-loaded niosomal hydrogel significantly reduced biofilm formation in the strains compared with free forms of metal NPs and CUR. Interestingly, compared with niosomal formulations, hydrogel-embedded niosomal formulations enhanced the inhibition zone and significantly decreased the minimal inhibitory and bactericidal concentrations. The cytotoxicity of the samples was analyzed by the tetrazolium (MTT) assay. The findings indicated that CUR-loaded niosomes exhibited the most negligible toxicity compared with the CUR-AgNP-loaded niosomal hydrogel and CUR-CuNP-loaded niosomal hydrogel at the same concentration. Moreover, the formulations of CUR-AgNP-loaded niosomes and CUR-CuNP-loaded niosomes displayed higher cytotoxicity than their hydrogel-incorporated counterparts (Fig. 12). It is worth noting

that niosomal CUR demonstrated lower cytotoxicity than free CUR, possibly attributed to variances in intracellular trafficking or diverse cellular uptake mechanisms between niosomal and free forms.

### 5.3. *Leishmania*

Leishmaniasis is one of the commonly neglected health problems caused by various species of *Leishmania*, and is endemic in the tropics and sub-tropics region. Pentavalent antimonials (SbV) are the first-line therapy for treating all forms of *Leishmania*. On the other hand, all current treatments have different drawbacks, such as high cost, severe side effects, drug resistance, dosage and duration of drug therapy, suboptimal treatment, and pharmacological deficiencies. Therefore, these limitations emphasize a requirement for more impressive treatment conditions and the progress of novel drugs or combination treatments against leishmaniasis. Mostafavi *et al.* investigated the loading of amphotericin B (AmB) and Glucantime in niosomes to treat cutaneous leishmaniasis through *in vitro* and *in vivo* studies.<sup>191</sup> In this research, the efficacy of the niosomal formulations of Glucantime and AmB, simple forms alone and in combination, were compared with free solutions of drugs. An MTT assay, gene expression profiling flow cytometry, and macrophage model were used to examine the as-prepared niosomal formulations' efficacy. The spleen's lesion size and parasite number were evaluated to assess the therapeutic influence of dual drug niosome on the lesion induced using *Leishmania major* in inbred BALB/c mice. Compared with free solutions of drugs, the niosomal formu-

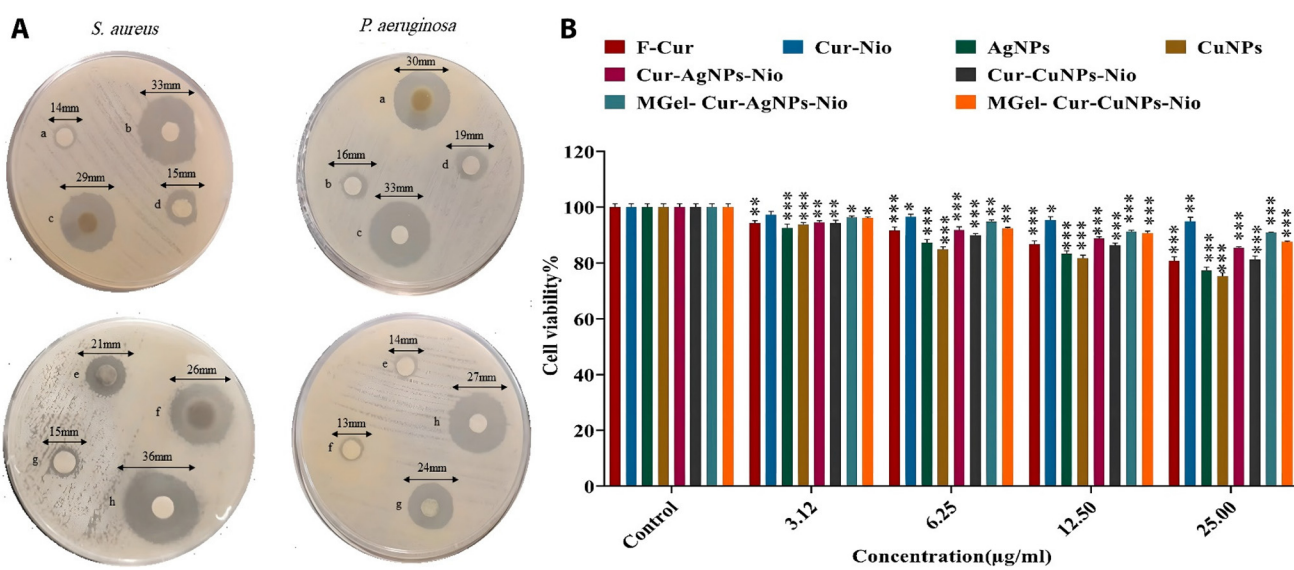


**Fig. 12** (A) *S. aureus* (left) and *Pseudomonas aeruginosa* (PA) (right) inhibit drug-free and drug-loaded zones. Left side: (a) pure curcumin, (b) curcumin-AgNP-laden niosomal hydrogel, curcumin-CuNP-containing niosomes, (d) copper NPs, (e) curcumin-laden niosomes, (f) niosomes laden with curcumin-AgNPs, (g) NPs of silver, and (h) curcumin-CuNP-infused niosomal hydrogel. The right side: (a) curcumin-AgNP-laden niosomal hydrogel, (b) copper NPs, (c) curcumin-CuNP-laden niosomal hydrogel, (d) curcumin-laden niosomes, (e) silver NPs, (f) free curcumin, curcumin-AgNP-laden niosomes, as well as curcumin-CuNP-containing niosomes. (B) *In vitro* cytotoxicity of HFF cells. FreeNio: niosomes that have been loaded with curcumin, Cur-AgNPs-Nio: niosomes that have been loaded with curcumin and AgNPs, Cur-CuNPs: niosomes that have been loaded with curcumin and CuNPs, niosomal hydrogel containing curcumin-CuNPs is known as MGel-Cur-AgNPs-Nio. Results are presented as mean, and standard deviation, with  $n = 3$ . \*\*\* $P < 0.001$ , \*\* $P < 0.01$ , \* $P < 0.05$ . Reproduced from ref. 190 with permission from [Elsevier], copyright [2021].

lations exhibited more significant inhibitory influences. The niosomal formulation of Glucantime and AmB exhibited an enhancement in the number of apoptotic cells and the levels of gene expression of IL-12 and metacaspase and a decline in IL-10 levels with a dose-response influence.

In other research, Mostafavi *et al.* reported selenium and Glucantime-loaded niosomes as a novel niosomal formulation against *Leishmania tropica*.<sup>192</sup> The efficacy of dual drug-loaded niosomes was compared with their simple forms alone. For evaluation of the effectiveness of novel niosomal formulations, an *in vitro* MTT test, gene expression profile, and intra-macrophage model were used. The results showed that no cytotoxicity effect has appeared for niosomal formulations of selenium and Glucantime, alone and in combination, and simple forms of selenium and Glucantime. Furthermore, niosomal formulations of the forms of selenium and Glucantime exhibited more inhibitory effects than the simple forms of selenium and Glucantime. Also, the levels of gene expression of interleukin (IL-10) reduced, while the level of IL-12 and metacaspase enhanced. Bahraminejad *et al.* prepared a dual zirconium/tioxolone niosomal formulation *via* a film hydration procedure, and its leishmanicidal performance against amastigotes and promastigotes was evaluated by MTT and flow cytometry methods.<sup>193</sup> Furthermore, apoptosis, gene expression levels, superoxide dismutase activity, the production of reactive oxygen species, and nitrite generation were studied to evaluate the mechanism of action niosomal formulation. The niosomal formulation of zirconium/tioxolone exhibited no cytotoxic effect. It increased the interleukin (IL)-12 expression level and inducible nitric oxide synthase and remarkably decreased the IL-10 gene expression level, which confirms the immunomodulatory role of zirconium/tioxolone niosomes.

Hakimi Parizi *et al.* reported niosomal formulations of tioxolone coupled with benzoxonium chloride against *Leishmania tropica*.<sup>194</sup> This research evaluated the leishmanicidal activity against amastigotes and promastigotes, apoptosis, gene expression levels of free tioxolone and benzoxonium chloride, and dual niosomal formulations of tioxolone and benzoxonium chloride. The niosomal formulations of tioxolone and benzoxonium chloride were more efficient than Glucantime on promastigotes and amastigotes. Furthermore, the toxicity of the prepared niosomal formulation was remarkably less than Glucantime. Also, the flow cytometry test on the dual niosome of tioxolone and benzoxonium chloride exhibited a higher number of early apoptotic events as the principal mode of action. Furthermore, the niosomal formulations enhanced the IL-12 expression level and metacaspase genes and reduced the IL-10 gene expression level. Anjum *et al.* designed AmB/pentamidine (PTM) niosomes and optimized them by the Box-Behnken design method.<sup>195</sup> The optimized AmB/PTM niosomes were incorporated into the chitosan. The as-synthesized AmB/PTM/niosome/gel increases the retention time of nano-carriers at the infection site and enables AmB/PTM niosomes to penetrate layers of skin. To analyze the release pattern of AmB and pentamidine, their *in vitro* release from AmB/PTM niosomes and AmB/PTM/niosome/gel was performed. The

results showed a prolonged release property compared with their respective drug solution. The results of the *ex vivo* permeation study showed a greater percentage inhibition, higher skin penetration, and lower IC<sub>50</sub> against the promastigotes of AmB/PTM niosomes, confirming its better antileishmanial activity.

#### 5.4. *Klebsiella pneumoniae*

*Klebsiella pneumoniae* is a Gram-negative bacterium causing catheter-related biofilm infections. Antimicrobial resistance in *Klebsiella pneumonia* is a major therapeutic challenge that needs to be resolved. Akbarzadeh *et al.* loaded gentamicin and ethylenediaminetetraacetic acid (EDTA) into niosomes to investigate the antibacterial performance and biofilm inhabitation against *Klebsiella pneumoniae* strains.<sup>196</sup> Various formulations of gentamicin/EDTA niosomes were fabricated by a thin-film hydration procedure. The properties of gentamicin/EDTA niosomes were optimization by Design-Expert software. Also, molecular docking was applied to assess the antibacterial activity of gentamicin. The niosomal formulation exhibited a prolonged drug release and high stability. The agar well diffusion method, minimum inhibitory concentration, and minimum bactericidal concentration were applied to evaluate the antimicrobial activity of gentamicin and EDTA-loaded niosomes. The results showed a good antimicrobial performance of niosomal formulations. Also, the crystal violet assay, biofilm gene expression assay, and minimum biofilm eradication concentration showed good anti-biofilm inhibitory influences of niosomal formulations.

#### 5.5. *Acinetobacter baumannii*

*Acinetobacter baumannii* is one of the worldwide health problems because of its high antibiotic resistance and capability to create biofilms. Shamkani *et al.* loaded minocycline and gallium nitrate into niosomes and validated the anti-biofilm activity toward *Acinetobacter baumannii*.<sup>197</sup> In order to form an aqueous polymer solution, polyethylene glycol and polyvinylpyrrolidone were incorporated into the as-prepared niosomal formulation. Entrapment efficiencies for gallium nitrate and minocycline niosomal formulations were 42.5 and 81.5%, respectively. The obtained release rate of niosomes containing gallium nitrate and minocycline was 20 and 50%, respectively. *In vitro* and *in vivo* analysis confirmed the superior anti-biofilm activity of the dual niosomes compared with non-niosomal compounds. Their livers and spleens were examined to determine whether the materials used were harmful to mice. Despite the excellent biofilm performance, niosomal formulations have a lower cytotoxic effect than the substances alone.

#### 5.6. Fungal keratitis

El-nabarawi *et al.* prepared natamycin-loaded niosomes incorporated into anti-inflammatory ketorolac tromethamine gel to improve the natamycin's clinical efficacy by increasing its penetration *via* corneal tissue and decreasing the inflammation associated with fungal keratitis.<sup>198</sup> The as-prepared niosomes showed a high entrapment efficiency of up to

96.43%. Compared with the marketed product and/or natamycin entrapped in niosomal formulations, the natamycin/niosomes/ketorolac tromethamine gel exhibited *in vitro* retardation of release. *In vivo* studies revealed the superiority of the niosomal formulation entrapped in ketorolac tromethamine gel and better effects on corneal infiltration and hypopyon level.

Bacterial resistance to multiple antibiotics is a significant concern in the field of global public health. This resistance causes antibacterial treatments to fail and infectious diseases to develop. Innovative approaches have been investigated to address bacterial infections. These include the co-administration of D-cycloserine and ethionamide, the encapsulation of ceftriaxone sodium and rifampicin within niosomes, and the utilization of chitosan gel-embedded niosomes laden with moxifloxacin for topical antimicrobial delivery. Notwithstanding this, the efficacy and enduring consequences of these methodologies remain incompletely comprehended.<sup>199</sup> The management of diseases such as *MT*, *PA*, *SA*, and leishmaniasis represents an additional obstacle. Although niosomes and combination therapies have been suggested as potential approaches to address the issue of antibiotic resistance exhibited by biofilm-forming bacteria and drug-resistant *MT*, *PA*, and *SA*, respectively, the effectiveness of these treatments is still being studied.<sup>200</sup> The existing therapeutic approaches for leishmaniasis, a prevalent health concern induced by diverse species of leishmania, are accompanied by several limitations: exorbitant expenses, severe adverse effects, drug resistance, suboptimal treatment efficacy, prolonged therapy duration, and pharmacological inadequacies. The injection of amphotericin B (AmB) and Glucantime into niosomes for the treatment of cutaneous leishmaniasis has been the subject of research. However, the precise inhibitory effects of these treatments remain to be determined.<sup>201</sup> Finally, antimicrobial resistance poses a significant therapeutic challenge for *Klebsiella pneumoniae*. Although scientists have loaded niosomes with gentamicin and ethylenediaminetetraacetic acid (EDTA) to examine their biofilm inhabitation and antibacterial activity against *Klebsiella pneumoniae* strains, the antimicrobial and anti-biofilm inhibitory effects of these niosomal formulations have not yet been validated.<sup>202</sup>

## 6. Other therapeutic purposes

In recent years, niosomes have been extensively investigated to treat various diseases, including Alzheimer's disease, diabetes, and HIV. For example, Kulkarni *et al.* loaded rivastigmine and *N*-acetyl cysteine into a niosomal nanocarrier to treat Alzheimer's disease.<sup>203</sup> The Box-Behnken experimental design was used to optimize the nanoniosomal formulations. Rivastigmine/*N*-acetyl cysteine niosomes exhibited a prolonged release of drug pattern for up to 2 days. DPPH radical scavenging and acetylcholinesterase enzyme inhibition tests revealed a better combinative influence than the free solution of drugs.

A 2-day nasal permeation confirmed the efficiency and biocompatibility of the prepared niosomal formulations. *In vivo* pharmacokinetic and organ biodistribution investigations showed a better drug profile and greater niosome distribution in the brain than in other organs. Developing efficient DDSs for treating diabetes is still in progress.<sup>204</sup> The most crucial factor in treating diabetes is maintaining blood glucose levels in a healthy range, regulated either through the direct entry of the hormone insulin into the body or through the consumption and injection of drugs. Using drugs in high dosages is necessary for a better control of the blood glucose level, which leads to harmful side effects on the human body. Therefore, the application of nanotechnology for the development of various formulations is essential. Samed *et al.* prepared novel niosomes for loading glipizide and metformin HCl to treat diabetes.<sup>205</sup> The niosomes were synthesized by thin film hydration procedure. Metformin HCl was entrapped in the inner core of the niosomes as a hydrophilic drug, while glipizide was encapsulated in the bilayers of the niosomes as a hydrophobic drug. The results of drug release studies showed a linear profile up to 8–10 h and lasting for about 12–14 hours for both metformin HCl and glipizide and drugs.

Porkoláb *et al.* examined the loading of alanine and glutathione in niosomes to deliver a protein cargo into cultured cells of the neurovascular unit.<sup>206</sup> In this study, the results demonstrated that using alanine/glutathione niosomal formulations led to increased cargo delivery into the neurovascular unit and astroglial cells. Moreover, when metabolic and endocytic inhibitors were employed, it was observed that the cellular uptake of niosomal formulations was partially mediated through endocytosis. Among the alanine transporter genes, the small neutral amino acid transporter SNAT2 (SLC38A2) exhibited high expression in all cell types except for SH-SY5Y neurons. The neutral amino acid transporter genes ASCT1 (SLC1A4) and ASCT2 (SLC1A5), as well as SNAT1 (SLC38A1), showed moderate expression levels. On the other hand, SNAT5 (SLC38A5) expression was found to be low-to-moderate in all tested cell types.

In another report, Mészáros *et al.* loaded glutathione and solute carrier ligands, including alanine and glucopyranose, into niosomes.<sup>207</sup> Loading targeting ligands on the niosomal formulations enhanced the cargo molecule uptake in cultured brain endothelial cells. The cellular uptake depends on temperature and is reduced by endocytosis blockers and metabolic inhibitors. The niosomal formulations enhanced the plasma membrane fluidity, revealing the fusion of nanovesicles with endothelial cell membranes. The application of cell-penetrating peptides like TAT ((AYGRKKRRQRRR)) for cellular transportation improvement has been widely considered. Yadavar-Nikravesh *et al.* loaded an anti-HIV drug (tenofovir) into a PEGylated niosomal formulation by a thin-film hydration procedure.<sup>208</sup> After that, the TAT peptide is embedded in the niosomal formulation. The as-prepared niosomal formulation exhibited a good entrapment efficiency of  $75 \pm 2.516\%$ . The MTT assay was employed to analyze the cytotoxic effects of different formulations, namely the PEGylated NP, tenofovir-

loaded PEGylated NP, free drug, tenofovir-loaded TAT-conjugated NP, and TAT peptide. All the treatments demonstrated concentration-dependent cytotoxicity on HeLa cells. Notably, the tenofovir-loaded TAT-conjugated NP exhibited a higher cytotoxic effect than the tenofovir-loaded PEGylated NP. Furthermore, the inhibitory effects of the samples against HIV-infected HeLa cells were investigated at various non-toxic dosages. The anti-Scr HIV-1 effects of all treatments followed a concentration-dependent pattern. Combining both the tenofovir-loaded TAT-conjugated NP and the tenofovir-loaded PEGylated NP demonstrated more potent inhibitory effects than free tenofovir at different concentrations. However, it was observed that the tenofovir-loaded TAT-conjugated NP exhibited weaker anti-HIV-1 effects than the tenofovir-loaded PEGylated NP. The results obtained from this study revealed a lower anti-Scr HIV effect, higher cytotoxicity, and improved release of tenofovir for the tenofovir-loaded TAT-conjugated PEGylated NP when compared with the PEGylated NP.

It is critical to emphasize that niosome stability is an initial consideration. Due to the aggregation, fusion, and leakage of the encapsulated drug that can occur as a result of their fluid bilayer structure, their shelf life, storage conditions, and biological activity may be adversely affected.<sup>209</sup> Expanding the manufacturing capacity of niosomes poses an additional obstacle. The preparation methods commonly employed are intended for laboratory-scale operations and may not be viable for large-scale manufacturing on account of cost, yield, and reproducibility concerns.<sup>209</sup> Targeting represents an additional substantial obstacle in the application of niosomes. Although medications can be passively targeted to specific tissues or organs, it may not always be possible to deliver them specifically and exclusively to the intended cells or receptors.<sup>210</sup> Lastly, niosome toxicity is a significant concern. The concentration, charge, and structure of particular surfactants utilized in niosomes may lead to cytotoxic, hemolytic, or irritant effects. As a result, a meticulous selection and optimization of surfactants and their mixtures are required.<sup>211</sup>

## 7. Challenges and future directions

Nanosomal co-delivery methods have several advantages. They may target various cancer cell pathways and processes with several drugs, improving effectiveness and overcoming multi-drug resistance.<sup>212</sup> These systems shield the transported chemicals from degradation and clearance, improve their solubility and permeability, and target the tumor location to release medications in a controlled manner.<sup>213</sup> This increases the stability and delivery efficiency and minimizes the therapeutic drug dose and frequency, preventing effects on normal tissues and organs.<sup>209</sup> This reduces toxicity and negative effects.<sup>214</sup> Furthermore, these systems are adaptable. They may be tailored to treatment drugs, tumor types, and patient conditions. Their functional components might include targeted ligands, stimulus-responsive materials, and imaging agents.<sup>113</sup>

Despite extensive research in the field of dual-niosomes as a controlled DDS to treat a wide range of diseases due to multiple advantages such as chemical stability, biocompatibility, and biodegradability, the application of targeted niosome formulations towards clinical usage has been limited. The different affinity of the drugs towards the niosomes is one of the main challenges for the dual-functional drug niosomes.<sup>205</sup> Therefore, the choice of amphiphilic molecules to prepare niosomes is significant because it provides various structural compartments to interact with the hydrophobic and hydrophilic drugs.<sup>215</sup> Leakage of drugs, a low EE, the short shelf life of the formulation, aggregation, fusion, hydrolysis of encapsulated drugs, and carrier stability are the other limitations that hinder the use of dual-niosomes as potential DDSs. Membrane filtration and heat sterilization are unsuitable for dual-niosomes. So, these challenges require further study to prepare commercially dual-functional drug niosomes. There are two methods to improve the dual-niosome stability at ambient conditions.<sup>42</sup> Dispersing dual-niosomes in a viscous gel is applied either to decrease the rapid leakage of the loaded drugs from niosomal formulations or to decrease the effect of a burst release perceived with dual-niosomes.<sup>216</sup> However, the release of drugs from this system may be complex because the molecules of drugs have to be released from the bilayer membranes and diffuse *via* the viscous gel.

Another procedure for better physical stability is using freeze-drying or spray-drying methods to convert the dual-niosomal liquid dispersion to a powder form. This approach increases the physical stability of the dual-niosomes and can also decrease the oxidative instability of oxidizable drug molecules by reducing the formation of hydroxyl free radicals. Sterilization of lipid-based products such as niosomes is a challenging effort. Steam sterilization and dry heat are inappropriate for lipid-based DDSs, as this may lead to an extensive leakage of drug molecules from the bilayer vesicles. Furthermore, membrane filtration is unsuitable for drug delivery formulations larger than the pore size of the bacterial filters. Fabrication of dual-niosomes under gas (ethylene oxide), gamma irradiation, and aseptic conditions can be suitable, as minimum heat is produced within the sterilization procedure. To sterilize the dual-niosomes, all the raw materials, including drug solutions, organic lipids, and buffer, are passed from the bacterial filters, and the final formulation is prepared under aseptic conditions. Gamma irradiation could be used for a packaged product and is applicable for heat-sensitive drugs due to its high penetration power. The sterilization of dual-niosome formulations with gamma irradiation is a useful method, and thus the influence of gamma illumination on the physical stability of dual-niosomes can be a potential investigative line for future work.

The building components of dual-niosomes are surfactants, which play critical roles in the preparation and properties of these DDSs. The usage of surfactants can lead to some degree of toxicity. However, no specific studies have been conducted to investigate the toxicity of these formulations in animal models, particularly in long-term investigations. It is crucial to

**Table 5** Nanosomal drug delivery methods' pros, cons, and prospective solutions for drug stability and targeted distribution

Challenge and future direction	Limitations	Solutions	Ref.
Drug affinity towards niosome	Variability in drug affinity towards niosomes	Selection of amphiphilic molecules for niosome preparation to interact with hydrophobic and hydrophilic drugs	217 and 218
Leakage of drugs	Low encapsulation efficiency (EE)	Incorporating dual-niosomes in a viscous gel to reduce rapid leakage and burst release, or utilizing freeze-drying or spray-drying methods to convert liquid dispersion to powder form	219 and 220
Formulation stability	Aggregation, fusion, hydrolysis, and short shelf life	Further research on stability enhancement methods such as freeze-drying, spray-drying, and sterility through gamma irradiation or aseptic conditions	221 and 222
Toxicity of surfactants	Lack of toxicity studies	Thorough investigation of long-term tolerability of surfactant-based systems in animal models before clinical application	209
Mass production	Infeasibility of mass-producing dual-drug carriers using current methods	Establishment of an efficient and cost-effective method for mass-producing dual-niosomes with uniform size and clinically acceptable properties	36

address this research gap and thoroughly examine the long-term tolerability of surfactant-based systems before they can be applied in clinical settings. Furthermore, there is a lack of sufficient attention given to exploring the potential applications of amphiphilic molecules, which possess biological activity or can serve as targetable ligands in bilayer vesicles. However, a few compounds with dual properties like biological activity and amphiphilicity may be available. So, preparing these amphiphilic compounds that could be converted into bilayer vesicles for the simultaneous delivery of two drugs is effective.

The development of appropriate dual-niosomes requires deliberation. The formulation of niosomes is influenced by a variety of factors, including the surfactant employed, the variables of production, and the method of preparation. Most presently employed, clinically acceptable nanotherapies have a simple structure and composition that lends itself well to mass production methods. The preponderance of dual-niosomes has been produced using conventional methods, such as reverse-phase evaporation, ether injections, and thin-film rehydration techniques. This method has a number of disadvantages, including the need to remove organic solvents, expensive costs, and a lengthy process. The laboratory production and analysis of dual-niosomes are typically performed on a milliliter scale. These small quantities are adequate for both *in vitro* and *in vivo* research. Dual-niosomes may be challenging to construct on a large scale due to the impossibility of mass-producing dual-drug carriers using current production methods. Therefore, it is essential to establish an efficient and cost-effective method for mass-producing dual-niosomes that are uniform in size and possess clinically acceptable properties. A comprehensive summary of the primary benefits, drawbacks, and possible remedies of nanosomal drug delivery systems is presented in Table 5. This entails an exhaustive examination of the advantages and disadvantages of these systems, including potential toxicity and difficulties in large-scale production, in addition to the benefits they provide, such as enhanced drug stability and targeted delivery. The table additionally examines possible approaches to surmount these

obstacles, providing an impartial viewpoint on the implementation of nanosomal drug delivery systems in therapeutic contexts.

## 8. Conclusion

In conclusion, nanoniosome-based medication codelivery systems have demonstrated therapeutic potential. A review of recent advancements in this field reveals the growth of nanotechnology in medicine, with a particular emphasis on cancer therapy. Nanosystems such as niosomes offer significant benefits for treating cancer and other diseases by increasing the solubility and stability of entrapped anticancer and antimicrobial medications. Due to their structure, sensitivity to pH changes, and ability to be functionalized, niosomes, a type of nanodelivery technology, have demonstrated great promise in the delivery of specific pharmaceuticals. The ability of niosomal formulations to permit combination therapy by co-delivering multiple drugs is one of its primary advantages. This includes the codelivery of chemotherapeutic agents, bioactive molecules, organic compounds, DNA, siRNA, and miRNA, among other substances. Recent research has examined in depth the use of dual-responsive niosomes for both drug delivery and cancer therapy. Niosomal DDSs can be classified according to their various forms, chemical compositions, and fabrication procedures. Methods for preparing niosomes include thin layer injections, ether injections, microfluidization, transmembrane pH gradients, the "bubble" technique, and others. These methods offer various advantages and considerations for the stability and structure of niosomal vesicle membranes. Dual niosomes have been utilized effectively in treating cancer to deliver two concurrent medications or a drug containing bioactive compounds derived from plants. Niosomes have also been utilized to transport drugs alongside gene agents, including siRNA, microRNA, shRNA, lncRNA, and DNA. Metallic niosomal carriers are also investigated for targeted distribution to enhance therapeutic efficacy. In addition to cancer therapy, dual-niosomes have shown promise in treat-

ing several diseases, including leishmanial infections, *PA*, and *MT* infections. Difficult tasks in the field include optimizing formulation characteristics, enhancing stability, overcoming biological barriers, and ensuring safe and efficient distribution. Current advancements in nanomiosome-based drug-combination systems emphasize their immense potential for therapeutic applications. Through continued research and development in this field, it will be possible to address these issues and pave the way for future advances in drug delivery and individualized treatment.

## Author contributions

Conceptualization, S. S.; writing – original draft preparation, M. R., A. D., H. M., E. B.-M.; writing – review and editing, S. F.-K., S. M., M. B.; supervision, S. S., M. B. All authors have read and agreed to the published version of the manuscript.

## Conflicts of interest

The authors declare that there is no conflict of interest regarding the publication of this article.

## References

- 1 L. Zhang, S. Deng, Y. Zhang, Q. Peng, H. Li, P. Wang, X. Fu, X. Lei, A. Qin and X. Yu, *Adv. Healthcare Mater.*, 2020, **9**, 1900772.
- 2 X. Lei, Z. Li, Y. Zhong, S. Li, J. Chen, Y. Ke, S. Lv, L. Huang, Q. Pan and L. Zhao, *Acta Pharm. Sin. B*, 2022, **12**, 3877–3890.
- 3 B. He, Y. Zhang, Z. Zhou, B. Wang, Y. Liang, J. Lang, H. Lin, P. Bing, L. Yu and D. Sun, *Front. Bioeng. Biotechnol.*, 2020, **8**, 737.
- 4 Y. Wang, W. Zhai, J. Li, H. Liu, C. Li and J. Li, *Tribol. Int.*, 2023, **188**, 108891.
- 5 S. Huang, J. Yuan, Y. Xie, K. Qing, Z. Shi, G. Chen, J. Gao, H. Tan and W. Zhou, *Cancer Nanotechnol.*, 2023, **14**, 1–15.
- 6 A. Mirzaiebadizi, H. Ravan, S. Dabiri, P. Mohammadi, A. Shahba, M. Ziasistani and M. Khatami, *Bioprocess Biosyst. Eng.*, 2022, **45**, 1781–1797.
- 7 L. Yan, J. Shen, J. Wang, X. Yang, S. Dong and S. Lu, *Dose-Response*, 2020, **18**, 1559325820936161.
- 8 A. Mitra, A. Nan, B. R. Line and H. Ghandehari, *Curr. Pharm. Des.*, 2006, **12**, 4729–4749.
- 9 S. Alikhanzadeh-Arani, M. Almasi-Kashi, S. Sargazi, A. Rahdar, R. Arshad and F. Baino, *Appl. Sci.*, 2021, **11**, 5339.
- 10 M. Razlansari, F. Ulucan-Karnak, M. Kahrizi, S. Mirinejad, S. Sargazi, S. Mishra, A. Rahdar and A. M. Diez-Pascual, *Eur. J. Pharm. Biopharm.*, 2022, 1–23.
- 11 U. Laraib, S. Sargazi, A. Rahdar, M. Khatami and S. Pandey, *Int. J. Biol. Macromol.*, 2022, **195**, 356–383.
- 12 H. Hosseinkhani and Y. Tabata, *J. Nanosci. Nanotechnol.*, 2006, **6**, 2320–2328.
- 13 R. Arshad, I. Fatima, S. Sargazi, A. Rahdar, M. Karamzadeh-Jahromi, S. Pandey, A. M. Diez-Pascual and M. Bilal, *Nanomaterials*, 2021, **11**, 3330.
- 14 S. Sargazi, M. Mukhtar, A. Rahdar, M. Barani, S. Pandey and A. M. Diez-Pascual, *Int. J. Mol. Sci.*, 2021, **22**, 10319.
- 15 M. Haghigat, A. Naroie, A. Rezvani, M. Hakimi, H. Saravani, M. Darroudi, A. Amini, M. Sabaghan and M. Khatami, *BioNanoScience*, 2021, **11**, 696–702.
- 16 S. Sargazi, R. Arshad, R. Ghamari, A. Rahdar, A. Bakhshi, S. F. Karkan, N. Ajalli, M. Bilal and A. M. Diez-Pascual, *Cell Biol. Int.*, 2022, **46**, 1320–1344.
- 17 M. Qindeel, F. Sabir, S. Sargazi, V. Mohammadzadeh and S. I. Mulla, *J. Nanopart. Res.*, 2021, **23**, 1–27.
- 18 R. Arshad, S. Sargazi, I. Fatima, A. Mobashar, A. Rahdar, N. Ajalli and G. Z. Kyzas, *ChemistrySelect*, 2022, **7**, e202201271.
- 19 S. Fathi-Karkan, S. Mirinejad, F. Ulucan-Karnak, M. Mukhtar, H. G. Almanghadim, S. Sargazi, A. Rahdar and A. M. Diez-Pascual, *Int. J. Biol. Macromol.*, 2023, 124103.
- 20 A. Sani, M. Pourmadadi, M. Shaghaghi, M. M. Eshaghi, S. Shahmollaghamsary, R. Arshad, S. Fathi-karkan, A. Rahdar, S. Jadoun and D. I. Medina, *J. Drug Delivery Sci. Technol.*, 2023, 104642.
- 21 M. Azizi, M. Shahgolzari, S. Fathi-Karkan, M. Ghasemi and H. Samadian, *Wiley Interdiscip. Rev.: Nanomed. Nanobiotechnol.*, 2022, e1872.
- 22 R. Rajera, K. Nagpal, S. K. Singh and D. N. Mishra, *Biol. Pharm. Bull.*, 2011, **34**, 945–953.
- 23 D. B. Momekova, V. E. Gugleva and P. D. Petrov, *ACS Omega*, 2021, **6**, 33265–33273.
- 24 F. Mahdiun, S. Mansouri, P. Khazaeli and R. Mirzaei, *Microb. Pathog.*, 2017, **107**, 129–135.
- 25 M. Barani, M. R. Hajinezhad, F. Zargari, S. Shahraki, F. Davodabadi, S. Mirinejad, S. Sargazi, A. Rahdar and A. M. Diez-Pascual, *J. Drug Delivery Sci. Technol.*, 2023, **84**, 104505.
- 26 R. Sarkar, A. Pal, A. Rakshit and B. Saha, *J. Surfactants Deterg.*, 2021, **24**, 709–730.
- 27 A. Kauslya, P. D. Borawake, J. V. Shinde and R. S. Chavan, *J. Drug Delivery Ther.*, 2021, **11**, 162–170.
- 28 S. Sargazi, M. Barani, F. Zargari, R. Arshad and R. K. Sharma, *Curr. Appl. Sci.*, 2022, 31–48.
- 29 J. Akbari, M. Saeedi, R. Enayatifard, K. Morteza-Semnani, S. M. H. Hashemi, A. Babaei, S. M. Rahimnia, S. S. Rostamkalei and A. Nokhodchi, *J. Drug Delivery Sci. Technol.*, 2020, **60**, 102035.
- 30 S. Agarwal, M. S. Mohamed, S. Raveendran, A. K. Rochani, T. Maekawa and D. S. Kumar, *RSC Adv.*, 2018, **8**, 32621–32636.
- 31 P. M. Gaafar, O. Y. Abdallah, R. M. Farid and H. Abdelkader, *J. Liposome Res.*, 2014, **24**, 204–215.
- 32 K. K. Patel, P. Kumar and H. P. Thakkar, *AAPS PharmSciTech*, 2012, **13**, 1502–1510.

33 P. Piplani, P. Kumar, A. Rohilla, S. Singla and I. P. Kaur, *Asian J. Biomed. Pharm. Sci.*, 2015, **5**, 8.

34 M. H. Nematollahi, A. Pardakhty, M. Torkzadeh-Mahanai, M. Mehrabani and G. Asadikaram, *RSC Adv.*, 2017, **7**, 49463–49472.

35 P. Bhardwaj, P. Tripathi, R. Gupta and S. Pandey, *J. Drug Delivery Sci. Technol.*, 2020, **56**, 101581.

36 D. Ag Selecí, M. Selecí, J.-G. Walter, F. Stahl and T. Schepers, *J. Nanomater.*, 2016, **2016**, 1–13.

37 K. M. Kazi, A. S. Mandal, N. Biswas, A. Guha, S. Chatterjee, M. Behera and K. Kuotsu, *J. Adv. Pharm. Technol. Res.*, 2010, **1**, 374.

38 S. Biju, S. Talegaonkar, P. Mishra and R. Khar, *Indian J. Pharm. Sci.*, 2006, **68**, 1–12.

39 S. Pacios-Michelena, J. D. García-García, R. Ramos-González, M. Chávez-González, E. I. Laredo-Alcalá, M. Govea-Salas, L. A. Menchaca-Castro, P. Segura-Ceníseros, A. Vargas-Segura and R. Arredondo-Valdes, *Bio-Based Nanoemulsions for Agri-Food Applications*, 2022, pp. 413–439.

40 M. A. Mavaddati, F. Moztarzadeh and F. Baghbani, *J. Cluster Sci.*, 2015, **26**, 2065–2078.

41 V. B. Junyaprasert, V. Teeranachaideekul and T. Supaperm, *AAPS PharmSciTech*, 2008, **9**, 851–859.

42 H. Abdelkader, A. W. Alani and R. G. Alany, *Drug Delivery*, 2014, **21**, 87–100.

43 B. Kapoor, R. Gupta, M. Gulati, S. K. Singh, R. Khursheed and M. Gupta, *Adv. Colloid Interface Sci.*, 2019, **271**, 101985.

44 J. Wen, M. Al Gailani, N. Yin and A. Rashidinejad, *Emulsion-based Systems for Delivery of Food Active Compounds: Formation, Application, Health and Safety*, 2018, pp. 263–292.

45 R. Joy, J. George and F. John, *ChemistrySelect*, 2022, **7**, e202104045.

46 S. Moghassemi and A. Hadjizadeh, *J. Controlled Release*, 2014, **185**, 22–36.

47 I. Akbarzadeh, M. T. Yaraki, S. Ahmadi, M. Chiani and D. Nourouzian, *Adv. Powder Technol.*, 2020, **31**, 4064–4071.

48 S. Fathi Karkan, S. Davaran and A. Akbarzadeh, *Nanomed. Res. J.*, 2019, **4**, 209–219.

49 S. Sargazi, R. Saravani, J. Z. Reza, H. Z. Jaliani, S. Mirinejad, Z. Rezaei and S. Zarei, *EXCLI J.*, 2019, **18**, 485.

50 S. Kummar, H. X. Chen, J. Wright, S. Holbeck, M. D. Millin, J. Tomaszewski, J. Zweibel, J. Collins and J. H. Doroshow, *Nat. Rev. Drug Discovery*, 2010, **9**, 843–856.

51 M. Hemati, F. Haghirsadat, F. Yazdian, F. Jafari, A. Moradi and Z. Malekpour-Dehkordi, *Artif. Cells, Nanomed., Biotechnol.*, 2019, **47**, 1295–1311.

52 M. Ghaffari, S. M. Kalantar, M. Hemati, A. Dehghani Firoozabadi, A. Asri, A. Shams, S. Jafari Ghalekohneh and F. Haghirsadat, *Biotechnol. Lett.*, 2021, **43**, 981–994.

53 M. Hemati, F. Haghirsadat, F. Jafary, S. Moosavizadeh and A. Moradi, *Int. J. Nanomed.*, 2019, 6575–6585.

54 S. Naderinezhad, G. Amoabediny and F. Haghirsadat, *RSC Adv.*, 2017, **7**, 30008–30019.

55 V. Gugleva, V. Michailova, R. Mihaylova, G. Momekov, M. M. Zaharieva, H. Najdenski, P. Petrov, S. Rangelov, A. Fors and B. Trzebicka, *Pharmaceutics*, 2022, **14**, 747.

56 A. Babu, A. Munshi and R. Ramesh, *Drug Dev. Ind. Pharm.*, 2017, **43**, 1391–1401.

57 P. Kulkarni and D. Rawtani, *J. Pharm. Sci.*, 2019, **108**, 2643–2653.

58 S. Yasamineh, P. Yasamineh, H. G. Kalajahi, O. Gholizadeh, Z. Yekanipour, H. Afkhami, M. Eslami, A. H. Kheirkhah, M. Taghizadeh and Y. Yazdani, *Int. J. Pharm.*, 2022, 121878.

59 G. John, P. Sinha, G. Rathnam, U. Ubaidulla and R. Aravind, *IOSR J. Pharm.*, 2021, **11**, 1–9.

60 M. Barani, F. Paknia, M. Roostaee, B. Kavyani, D. Kalantar-Neyestanaki, N. Ajalli and A. Amirbeigi, *BioMed Res. Int.*, 2023, **2023**, 1–9.

61 M. G. Umbarkar, *Indian J. Pharm. Educ. Res.*, 2021, **55**, s11–s28.

62 M. Yaghoobian, A. Haeri, N. Bolourchian, S. Shahhosseni and S. Dadashzadeh, *Int. J. Nanomed.*, 2020, 8767–8781.

63 B. A. Witika, K. E. Bassey, P. H. Demana, X. Siwe-Noundou and M. S. Poka, *Int. J. Mol. Sci.*, 2022, **23**, 9668.

64 R. Bartelds, M. H. Nematollahi, T. Pols, M. C. Stuart, A. Pardakhty, G. Asadikaram and B. Poolman, *PLoS One*, 2018, **13**, e0194179.

65 K. Mahmoud, M. Mohamed, I. Amr and L. Dina, *DDPIJ. MS. ID*, 2018, **125**, 9.

66 P. Tangri and S. Khurana, *Int. J.*, 2011, **2229**, 7499.

67 S. Kumavat, P. K. Sharma, S. S. Koka, R. Sharma, A. Gupta and G. Darwhekar, *J. Drug Delivery Ther.*, 2021, **11**, 208–212.

68 G. S. Myneni, G. Radha and G. Soujanya, *J. Pharm. Res.*, 2021, **11**, 1–12.

69 S. K. Ray, N. Bano, T. Shukla, N. Upmanyu, S. P. Pandey and G. Parkhe, *J. Drug Delivery Ther.*, 2018, **8**, 335–341.

70 S. Rane, Y. Inamdar, B. Rane and A. Jain, *Int. J. Pharm. Sci. Rev. Res.*, 2018, **51**, 198–213.

71 S. Durak, M. Esmaeili Rad, A. Alp Yetisgin, H. Eda Sutova, O. Kutlu, S. Cetinel and A. Zarrabi, *Nanomaterials*, 2020, **10**, 1191.

72 M. Schlich, F. Lai, R. Pireddu, E. Pini, G. Ailuno, A. Fadda, D. Valenti and C. Sinico, *Food Chem.*, 2020, **310**, 125950.

73 T. Yoshioka, N. Skalko, M. Gursel, G. Gregoriadis and A. T. Florence, *J. Drug Targeting*, 1995, **2**, 533–539.

74 X. Ge, M. Wei, S. He and W.-E. Yuan, *Pharmaceutics*, 2019, **11**, 55.

75 M. K. Waqas, H. Sadia, M. I. Khan, M. O. Omer, M. I. Siddique, S. Qamar, M. Zaman, M. H. Butt, M. W. Mustafa and N. Rasool, *Des. Monomers Polym.*, 2022, **25**, 165–174.

76 M. Masjedi and T. Montahaei, *J. Drug Delivery Sci. Technol.*, 2021, **61**, 102234.

77 A. Zaid Alkilani, H. Abu-Zour, A. Alshishani, R. Abu-Huwaij, H. A. Basheer and H. Abo-Zour, *Nanomaterials*, 2022, **12**, 3570.

78 M. A. Shewaiter, A. A. Selim, Y. M. Moustafa, S. Gad and H. M. Rashed, *Int. J. Pharm.*, 2022, **628**, 122345.

79 M. Matos, D. Pando and G. Gutiérrez, in *Lipid-based nano-structures for food encapsulation purposes*, Elsevier, 2019, pp. 447–481.

80 D. Ag Seleci, V. Maurer, F. Stahl, T. Scheper and G. Garnweitner, *Int. J. Mol. Sci.*, 2019, **20**, 4696.

81 A. D. Bangham, M. M. Standish and J. C. Watkins, *J. Mol. Biol.*, 1965, **13**, 1–13, 238-IN227.

82 A. Kalaiselvi, J. G. A. Jeno, S. M. Roopan, G. Madhumitha and E. Nakkeeran, *Int. Biodeterior. Biodegrad.*, 2019, **137**, 102–108.

83 J. G. Aswin Jeno, S. Maria Packiam and E. Nakkeeran, *Int. J. Trop. Insect Sci.*, 2022, **42**, 1373–1387.

84 A. Manosroi, R. Chutoprapat, M. Abe and J. Manosroi, *Int. J. Pharm.*, 2008, **352**, 248–255.

85 L. Baldino and E. Reverchon, *J. CO<sub>2</sub> Util.*, 2021, **52**, 101669.

86 D. Sharma, A. A. E. Ali and J. R. Aate, *PharmaTutor*, 2018, **6**, 58–65.

87 Y. Zhang, F. Cao and A. Ullah, *Mater. Today Commun.*, 2022, **31**, 103738.

88 M. Naghdi, M. Taheran, S. K. Brar, T. Rouissi, M. Verma, R. Y. Surampalli and J. R. Valero, *J. Cleaner Prod.*, 2017, **164**, 1394–1405.

89 L. Temprom, S. Krongsuk, S. Thapphasaraphong, A. Priperm and S. Namuangruk, *Mater. Today Commun.*, 2022, **31**, 103340.

90 M. Mokhtar, O. A. Sammour, M. A. Hammad and N. A. Megrab, *Int. J. Pharm.*, 2008, **361**, 104–111.

91 C. Kirby and G. Gregoriadis, *Bio/Technology*, 1984, **2**, 979–984.

92 P. Kallinteri, D. Fatouros, P. Klepetsanis and S. G. Antimisiaris, *J. Liposome Res.*, 2004, **14**, 27–38.

93 L. K. Yeo, C. S. Chaw and A. A. Elkordy, *Pharmaceuticals*, 2019, **12**, 46.

94 L. Wen, F. Cheng, Y. Zhou and C. Yin, *Saudi J. Gastroenterol.*, 2015, **21**, 313.

95 A. Alemi, J. Zavar Reza, F. Haghirladsadat, H. Zarei Jaliani, M. Hagh Karamallah, S. A. Hosseini and S. Hagh Karamallah, *J. Nanobiotechnol.*, 2018, **16**, 1–20.

96 J. M. Caster, M. Sethi, S. Kowalczyk, E. Wang, X. Tian, S. N. Hyder, K. T. Wagner, Y.-A. Zhang, C. Kapadia and K. M. Au, *Nanoscale*, 2015, **7**, 2805–2811.

97 J. R. Mackey, M. Martin, T. Pienkowski, J. Rolski, J.-P. Guastalla, A. Sami, J. Glaspy, E. Juhos, A. Wardley and T. Fornander, *Lancet Oncol.*, 2013, **14**, 72–80.

98 G. Minotti, S. Recalcati, P. Menna, E. Salvatorelli, G. Corra and G. Cairo, *Methods Enzymol.*, 2004, **378**, 340–361.

99 R. Muzzalupo, L. Tavano and C. La Mesa, *Int. J. Pharm.*, 2013, **458**, 224–229.

100 G. N. Devaraj, S. Parakh, R. Devraj, S. Apte, B. R. Rao and D. Rambhau, *J. Colloid Interface Sci.*, 2002, **251**, 360–365.

101 P. Kulkarni, D. Rawtani and T. Barot, *Colloids Surf. A*, 2019, **565**, 131–142.

102 H. Sahrayi, E. Hosseini, S. Karimifard, N. Khayam, S. M. Meybodi, S. Amiri, M. Bourbour, B. Farasati Far, I. Akbarzadeh and M. Bhia, *Pharmaceuticals*, 2021, **15**, 6.

103 A. Moammeri, K. Abbaspour, A. Zafarian, E. Jamshidifar, H. Motasadizadeh, F. Dabbagh Moghaddam, Z. Salehi, P. Makvandi and R. Dinarvand, *ACS Appl. Bio Mater.*, 2022, **5**, 675–690.

104 Z. A. Lalami, F. Tafvizi, V. Naseh and M. Salehipour, *J. Drug Delivery Sci. Technol.*, 2022, **72**, 103371.

105 D. H. Khan, S. Bashir, M. I. Khan, P. Figueiredo, H. A. Santos and L. Peltonen, *J. Drug Delivery Sci. Technol.*, 2020, **58**, 101763.

106 N. I. Mohamad Saimi, N. Salim, N. Ahmad, E. Abdulmalek and M. B. Abdul Rahman, *Pharmaceutics*, 2021, **13**, 59.

107 H. Wang, Q. Fan, L. Zhang, D. Shi, H. Wang, S. Wang and B. Bian, *Pteridines*, 2020, **31**, 158–164.

108 V. Talebi, B. Ghanbarzadeh, H. Hamishehkar, A. Pezeshki and A. Ostadrahimi, *J. Drug Delivery Sci. Technol.*, 2021, **61**, 101284.

109 A. H. Azandaryani, S. Kashanian, M. Shahlaei, K. Derakhshandeh, M. Motiei and S. Moradi, *Pharm. Res.*, 2019, **36**, 1–11.

110 A. Reis-Mendes, F. Carvalho, F. Remiāo, E. Sousa, M. d. L. Bastos and V. M. Costa, *Biomolecules*, 2019, **9**, 98.

111 E. Knyazev, S. Nikulin, A. Y. Khristichenko, T. Gerasimenko, O. Kindeeva, V. Petrov, G. Belyakova and D. Maltseva, *Russ. Chem. Bull.*, 2019, **68**, 2344–2349.

112 M. Moghtaderi, A. Mirzaie, N. Zabet, A. Moammeri, A. Mansoori-Kermani, I. Akbarzadeh, F. Eshrati Yeganeh, A. Chitgarzadeh, A. Bagheri Kashtali and Q. Ren, *Nanomaterials*, 2021, **11**, 1573.

113 P. Aparajay and A. Dev, *Eur. J. Pharm. Sci.*, 2022, **168**, 106052.

114 S. Dasari and P. B. Tchounwou, *Eur. J. Pharmacol.*, 2014, **740**, 364–378.

115 R. Roberts, L. Hanna, A. Borley, G. Dolan and E. M. Williams, *Eur. J. Cancer Care*, 2019, **28**, e13114.

116 L. S. Tarpgaard, C. Qvortrup, S. L. Nielsen, J. Stenvang, S. Detlefsen, N. Brünner and P. Pfeiffer, *Acta Oncol.*, 2021, **60**, 954–956.

117 E. Jamshidifar, F. Eshrati Yeganeh, M. Shayan, M. Tavakkoli Yaraki, M. Bourbour, A. Moammeri, I. Akbarzadeh, H. Noorbazargan and N. Hosseini-Khannazer, *Int. J. Mol. Sci.*, 2021, **22**, 7948.

118 L. Kanaani, M. M. Tabrizi, A. A. Khiyavi and I. Javadi, *Asian Pac. J. Cancer Biol.*, 2017, **2**, 27–29.

119 O.-C. Jeon, S. R. Hwang, T. A. Al-Hilal, J. W. Park, H. T. Moon, S. Lee, J. H. Park and Y. Byun, *Pharm. Res.*, 2013, **30**, 959–967.

120 M. I. Khan, A. Madni and L. Peltonen, *Eur. J. Pharm. Sci.*, 2016, **95**, 88–95.

121 S. Aryal, C.-M. J. Hu, V. Fu and L. Zhang, *J. Mater. Chem.*, 2012, **22**, 994–999.

122 N. Ferreira, N. P. Gonçalves, M. J. Saraiva and M. R. Almeida, *Sci. Rep.*, 2016, **6**, 26623.

123 X. Yang, Z. Li, N. Wang, L. Li, L. Song, T. He, L. Sun, Z. Wang, Q. Wu and N. Luo, *Sci. Rep.*, 2015, **5**, 1–15.

124 M. S. Zaman, N. Chauhan, M. M. Yallapu, R. K. Gara, D. M. Maher, S. Kumari, M. Sikander, S. Khan, N. Zafar and M. Jaggi, *Sci. Rep.*, 2016, **6**, 20051.

125 S. Barui, S. Saha, G. Mondal, S. Haseena and A. Chaudhuri, *Biomaterials*, 2014, **35**, 1643–1656.

126 D. A. Selecic, M. Selecic, F. Stahl and T. Scheper, *RSC Adv.*, 2017, **7**, 33378–33384.

127 M. Fatemizadeh, F. Tafvizi, F. Shamsi, S. Amiri, A. Farajzadeh and I. Akbarzadeh, *Iran. J. Pathol.*, 2022, **17**, 183.

128 I. Akbarzadeh, M. Fatemizadeh, F. Heidari and N. M. Nir, *Arch. Adv. Biosci.*, 2020, **11**, 1–9.

129 D. H. Khan, S. Bashir, A. Correia, M. I. Khan, P. Figueiredo, H. A. Santos and L. Peltonen, *Int. J. Pharm.*, 2019, **572**, 118764.

130 S. W. El-Far, H. A. Abo El-Enin, E. M. Abdou, O. E. Nafea and R. Abdelmonem, *Pharmaceuticals*, 2022, **15**, 816.

131 G. Maniam, C.-W. Mai, M. Zulkefeli and J.-Y. Fu, *Nanomedicine*, 2021, **16**, 373–389.

132 A. Firouzi Amandi, E. Jokar, M. Eslami, M. Dadashpour, M. Rezaie, Y. Yazdani and B. Nejati, *Med. Oncol.*, 2023, **40**, 170.

133 M. Bourbour, N. Khayam, H. Noorbazargan, M. T. Yaraki, Z. A. Lalami, I. Akbarzadeh, F. E. Yeganeh, A. Dolatabadi, F. M. Rad and Y. N. Tan, *Mol. Syst. Des. Eng.*, 2022, **7**, 1102–1118.

134 A. Bansal, D. Kapoor, R. Kapil, N. Chhabra and S. Dhawan, *Acta Pharm.*, 2011, **61**, 141–156.

135 D. N. Heo, D. H. Yang, H.-J. Moon, J. B. Lee, M. S. Bae, S. C. Lee, W. J. Lee, I.-C. Sun and I. K. Kwon, *Biomaterials*, 2012, **33**, 856–866.

136 C. Yang, T. Wu, Y. Qi and Z. Zhang, *Theranostics*, 2018, **8**, 464.

137 Z. Fan, B. Jiang, D. Shi, L. Yang, W. Yin, K. Zheng, X. Zhang, C. Xin, G. Su and Z. Hou, *Int. J. Pharm.*, 2021, **594**, 120184.

138 J. Dong, Z. Qin, W.-D. Zhang, G. Cheng, A. G. Yehuda, C. R. Ashby Jr., Z.-S. Chen, X.-D. Cheng and J.-J. Qin, *Drug Resist. Updates*, 2020, **49**, 100681.

139 H. Fasehee, R. Dinarvand, A. Ghavamzadeh, M. Esfandyari-Manesh, H. Moradian, S. Faghihi and S. H. Ghaffari, *J. Nanobiotechnol.*, 2016, **14**, 1–18.

140 F. Esmaeili, M. H. Ghahremani, S. N. Ostad, F. Atyabi, M. Seyedabadi, M. R. Malekshahi, M. Amini and R. Dinarvand, *J. Drug Targeting*, 2008, **16**, 415–423.

141 R. Ghafelehbashi, I. Akbarzadeh, M. T. Yaraki, A. Lajevardi, M. Fatemizadeh and L. H. Saremi, *Int. J. Pharm.*, 2019, **569**, 118580.

142 T. A. Yap, A. Omlin and J. S. De Bono, *J. Clin. Oncol.*, 2013, **31**, 1592–1605.

143 R. Tong and D. S. Kohane, *Annu. Rev. Pharmacol. Toxicol.*, 2016, **56**, 41–57.

144 B. Mansoori, S. S. Shotorbani and B. Baradaran, *Adv. Pharm. Bull.*, 2014, **4**, 313.

145 T. Golan, E. Z. Khvalevsky, A. Hubert, R. M. Gabai, N. Hen, A. Segal, A. Domb, G. Harari, E. B. David and S. Raskin, *Oncotarget*, 2015, **6**, 24560.

146 E. P. Pappou and N. Ahuja, *Gastrointest. Cancer Res.*, 2010, **S2**.

147 M. Sun, C. Yang, J. Zheng, M. Wang, M. Chen, D. Q. S. Le, J. Kjems and C. E. Bünger, *Acta Biomater.*, 2015, **28**, 171–182.

148 S. Filleur, A. Courtin, S. Ait-Si-Ali, J. Guglielmi, C. Merle, A. Harel-Bellan, P. Clézardin and F. Cabon, *Cancer Res.*, 2003, **63**, 3919–3922.

149 Z.-Y. Ding, H.-R. Wu, J.-M. Zhang, G.-R. Huang and D.-D. Ji, *Int. J. Clin. Exp. Pathol.*, 2014, **7**, 722.

150 M. G. Refolo, R. D'Alessandro, N. Malerba, C. Laezza, M. Bifulco, C. Messa, M. G. Caruso, M. Notarnicola and V. Tutino, *J. Cell. Physiol.*, 2015, **230**, 2973–2980.

151 S. Srivastava, R. R. Somasagara, M. Hegde, M. Nishana, S. K. Tadi, M. Srivastava, B. Choudhary and S. C. Raghavan, *Sci. Rep.*, 2016, **6**, 1–13.

152 R. B. Campbell, S. V. Balasubramanian and R. M. Straubinger, *Biochim. Biophys. Acta, Biomembr.*, 2001, **1512**, 27–39.

153 L. E. Rohde, N. Clausell, J. P. Ribeiro, L. Goldraich, R. Netto, G. W. Dec, T. G. DiSalvo and C. A. Polanczyk, *Int. J. Cardiol.*, 2005, **102**, 71–77.

154 D. Zhi, S. Zhang, B. Wang, Y. Zhao, B. Yang and S. Yu, *Bioconjugate Chem.*, 2010, **21**, 563–577.

155 E. Ojeda, G. Puras, M. Agirre, J. Zárate, S. Grijalvo, R. Pons, R. Eritja, G. Martínez-Navarrete, C. Soto-Sánchez and E. Fernández, *Org. Biomol. Chem.*, 2015, **13**, 1068–1081.

156 N. A. Abtahi, S. M. Naghib, S. J. Ghalekohneh, Z. Mohammadpour, H. Nazari, S. M. Mosavi, S. M. Gheibihayat, F. Haghjalsadat, J. Z. Reza and B. Z. Doulabi, *Chem. Eng. J.*, 2022, **429**, 132090.

157 Z. Salah, E. M. Abd El Azeem, H. F. Youssef, A. M. Gamal-Eldeen, A. R. Farrag, E. El-Meleigy, B. Soliman and M. Elhefnawi, *Curr. Gene Ther.*, 2019, **19**, 342–354.

158 N. A. Abtahi, S. Salehi, S. M. Naghib, F. Haghjalsadat, M. A. Edgahi, S. Ghorbanzadeh and W. Zhang, *Cancer Nanotechnol.*, 2023, **14**, 1–18.

159 W.-T. Guo and Y. Wang, *Cell. Mol. Life Sci.*, 2019, **76**, 1697–1711.

160 C.-S. Zhu, L. Zhu, D.-A. Tan, X.-Y. Qiu, C.-Y. Liu, S.-S. Xie and L.-Y. Zhu, *Comput. Struct. Biotechnol. J.*, 2019, **17**, 904–916.

161 N. A. Abtahi, S. M. Naghib, F. Haghjalsadat and M. Akbari Edgahi, *Cancer Nanotechnol.*, 2022, **13**, 1–18.

162 R. Aqeilan, G. Calin and C. Croce, *Cell Death Differ.*, 2010, **17**, 215–220.

163 M. Acunzo and C. M. Croce, *Clin. Chem.*, 2016, **62**, 655–656.

164 W. Kang, J. H. Tong, R. W. Lung, Y. Dong, J. Zhao, Q. Liang, L. Zhang, Y. Pan, W. Yang and J. Pang, *Mol. Cancer*, 2015, **14**, 1–10.

165 N. Patel, K. R. Garikapati, M. J. Ramaiah, K. K. Polavarapu, U. Bhadra and M. P. Bhadra, *Life Sci.*, 2016, **164**, 60–70.

166 C.-K. Cai, G.-Y. Zhao, L.-Y. Tian, L. Liu, K. Yan, Y.-L. Ma, Z.-W. Ji, X.-X. Li, K. Han and J. Gao, *Oncol. Rep.*, 2012, **28**, 1764–1770.

167 J. Liu, G. Chen, L. Feng, W. Zhang, H. Pelicano, F. Wang, M. A. Ogasawara, W. Lu, H. M. Amin and C. M. Croce, *Leukemia*, 2014, **28**, 118–128.

168 D. Bonci, V. Coppola, M. Musumeci, A. Addario, R. Giuffrida, L. Memeo, L. D'urso, A. Pagliuca, M. Biffoni and C. Labbaye, *Nat. Med.*, 2008, **14**, 1271–1277.

169 M. Gharbavi, B. Johari, E. Rismani, N. Mousazadeh, A. H. Taromchi and A. Sharafi, *ACS Chem. Neurosci.*, 2020, **11**, 4499–4515.

170 A. Bradshaw, A. Wickremsekera, S. T. Tan, L. Peng, P. F. Davis and T. Itinteang, *Front. Surg.*, 2016, **3**, 21.

171 N. Gawlik-Rzemieniewska and I. Bednarek, *Cancer Biol. Ther.*, 2016, **17**, 1–10.

172 I. Mahalaxmi, S. M. Devi, J. Kaavya, N. Arul, V. Balachandar and K. S. Santhy, *Eur. J. Pharmacol.*, 2019, **852**, 51–57.

173 S. Rezaei, A. Jalili, S. H. Aghaee-Bakhtiari and A. Sahebkar, *Drug Discovery Today*, 2020, **25**, 195–200.

174 M. Gharbavi, B. Johari, N. Mousazadeh, B. Rahimi, M. P. Leilan, S. S. Eslami and A. Sharafi, *Mol. Biol. Rep.*, 2020, **47**, 6517–6529.

175 S. Turker, A. Yekta Özer, E. Kılıç, M. Özalp, S. Colak and M. Korkmaz, *Interv. Med. Appl. Sci.*, 2013, **5**, 60–69.

176 I. Villate-Beitia, N. F. Truong, I. Gallego, J. Zárate, G. Puras, J. L. Pedraz and T. Segura, *RSC Adv.*, 2018, **8**, 31934–31942.

177 R. Falahat, M. Wiranowska, N. D. Gallant, R. Toomey, R. Hill and N. Alcantar, *Cell. Immunol.*, 2015, **298**, 96–103.

178 S. Karimifard, N. Rezaei, E. Jamshidifar, S. Moradi Falah Langeroodi, M. Abdihaji, A. Mansouri, M. Hosseini, N. Ahmadkhani, Z. Rahmati and M. Heydari, *ACS Appl. Nano Mater.*, 2022, **5**, 8811–8825.

179 M. Wiranowska, R. Singh, R. Falahat, E. Williams, J. O. Johnson and N. Alcantar, *Cancer Nanotechnol.*, 2020, **11**, 1–20.

180 A. Zarepour, A. C. Egil, M. Cokol Cakmak, M. Esmaeili Rad, Y. Cetin, S. Aydinlik, G. Ozaydin Ince and A. Zarrabi, *Polymers*, 2023, **15**, 298.

181 S. Salehi, M. S. Nourbakhsh, M. Yousefpour, G. Rajabzadeh and S. Sahab-Negah, *J. Microencapsulation*, 2022, **39**, 226–238.

182 A. Tambe and N. Pandita, *J. Drug Delivery Sci. Technol.*, 2018, **44**, 172–180.

183 F. Hosseini, M. M. Chegeni, A. Bidaki, M. Zaer, H. Abolhassani, S. A. Seyed, S. A. Nabipoorashrafi, A. A. Menarbazari, A. Moeinzadeh and A. R. Farmani, *Int. J. Biol. Macromol.*, 2023, 124697.

184 Y. Luo, X. Wei, Y. Wan, X. Lin, Z. Wang and P. Huang, *Acta Biomater.*, 2019, **92**, 37–47.

185 A. Y. Safhi, *Pharmaceuticals*, 2022, **15**, 678.

186 S. Han and J. Wu, *Bioact. Mater.*, 2022, 1–15.

187 G. Arslan Azizoglu, S. Tuncay Tanrıverdi, F. Aydin Kose, P. Ballar Kirmizibayrak and O. Ozer, *AAPS PharmSciTech*, 2017, **18**, 2987–2998.

188 X. Yang, Y. Tang, M. Wang, Y. Wang, W. Wang, M. Pang and Y. Xu, *Int. J. Pharm.*, 2021, **605**, 120826.

189 S. Sohrabi, A. Haeri, A. Mahboubi, A. Mortazavi and S. Dadashzadeh, *Int. J. Biol. Macromol.*, 2016, **85**, 625–633.

190 A. A. Targhi, A. Moammeri, E. Jamshidifar, K. Abbaspour, S. Sadeghi, L. Lamakani and I. Akbarzadeh, *Bioorg. Chem.*, 2021, **115**, 105116.

191 M. Mostafavi, I. Sharifi, S. Farajzadeh, P. Khazaeli, H. Sharifi, E. Pourseyedi, S. Kakooei, M. Bamorovat, A. Keyhani and M. H. Parizi, *Biomed. Pharmacother.*, 2019, **116**, 108942.

192 M. Mostafavi, S. Farajzadeh, I. Sharifi, P. Khazaeli and H. Sharifi, *J. Parasit. Dis.*, 2019, **43**, 176–185.

193 S. Bahraminejad, A. Pardakhty, I. Sharifi, M. Ranjbar, S. Karami-Mohajeri and F. Sharifi, *Arabian J. Chem.*, 2022, **15**, 104156.

194 M. H. Parizi, S. Farajzadeh, I. Sharifi, A. Pardakhty, M. H. D. Parizi, H. Sharifi, E. Salarkia and S. Hassanzadeh, *Korean J. Parasitol.*, 2019, **57**, 359.

195 A. Anjum, K. Shabbir, F. U. Din, S. Shafique, S. S. Zaidi, A. H. Almari, T. Alqahtani, A. Maryam, M. Moneeb Khan and A. Al Fatease, *Drug Delivery*, 2023, **30**, 2173335.

196 I. Akbarzadeh, N. Rezaei, S. Bazzazan, M. N. Mezajin, A. Mansouri, H. Karbalaeiheidar, S. Ashkezari, Z. S. Moghaddam, Z. A. Lalami and E. Mostafavi, *Biomater. Adv.*, 2023, **149**, 213384.

197 F. Shamkani, S. M. Barzi, F. Badmasti, M. Chiani, M. Zafari and M. Shafiei, *Int. Immunopharmacol.*, 2023, **115**, 109551.

198 M. A. El-Nabarawi, R. T. Abd El Rehem, M. Teaima, M. Abary, H. M. El-Mofty, M. M. Khafagy, N. M. Lotfy and M. Salah, *Drug Dev. Ind. Pharm.*, 2019, **45**, 922–936.

199 S. Sagar, S. Kaistha, A. J. Das and R. Kumar, *Antibiotic Resistant Bacteria: A Challenge to Modern Medicine*, Springer, 2019.

200 P. Minakshi, M. Ghosh, B. Brar, R. Kumar, U. P. Lambe, K. Ranjan, J. Manoj and G. Prasad, *Curr. Pharm. Des.*, 2019, **25**, 1554–1579.

201 E. B. Souto, J. Dias-Ferreira, S. A. Craveiro, P. Severino, E. Sanchez-Lopez, M. L. Garcia, A. M. Silva, S. B. Souto and S. Mahant, *Pathogens*, 2019, **8**, 119.

202 T. Piri-Gharaghie, N. Jegargoshe-Shirin, S. Saremi-Nouri, S.-H. Khademhosseini, E. Hoseinnezhad-Lazarjani, A. Mousavi, H. Kabiri, N. Rajaei, A. Riahi and A. Farhadi-Biregani, *Sci. Rep.*, 2022, **12**, 5140.

203 P. Kulkarni, D. Rawtani and T. Barot, *Eur. J. Pharm. Biopharm.*, 2021, **163**, 1–15.

204 M. Barani, S. Sargazi, V. Mohammadzadeh, A. Rahdar, S. Pandey, N. K. Jha, P. K. Gupta and V. K. Thakur, *J. Funct. Biomater.*, 2021, **12**, 54.

205 N. Samed, V. Sharma and A. Sundaramurthy, *Appl. Surf. Sci.*, 2018, **449**, 567–573.

206 G. Porkoláb, M. Mészáros, A. Tóth, A. Szecskó, A. Harazin, Z. Szegletes, G. Ferenc, A. Blastyák, L. Mátés and G. Rákely, *Pharmaceutics*, 2020, **12**, 635.

207 M. Mészáros, G. Porkoláb, L. Kiss, A.-M. Pilbat, Z. Kóta, Z. Kupihár, A. Kéri, G. Galbács, L. Siklós and A. Tóth, *Eur. J. Pharm. Sci.*, 2018, **123**, 228–240.

208 M.-S. Yadavar-Nikravesh, S. Ahmadi, A. Milani, I. Akbarzadeh, M. Khoobi, R. Vahabpour, A. Bolhassani and H. Bakhshandeh, *Adv. Powder Technol.*, 2021, **32**, 3161–3173.

209 M. Thakkar, *Curr. Drug Delivery*, 2016, **13**, 1275–1289.

210 C. Marianelli, L. Di Marzio, F. Rinaldi, C. Celia, D. Paolino, F. Alhaique, S. Esposito and M. Cara, *Adv. Colloid Interface Sci.*, 2014, **205**, 187–206.

211 A. R. Al Jayoush, H. A. Hassan, H. Asiri, M. Jafar, R. Saeed, R. Harati and M. Haider, *J. Drug Delivery Sci. Technol.*, 2023, 105007.

212 M. Moghtaderi, K. Sedaghatnia, M. Bourbou, M. Fatemizadeh, Z. Salehi Moghaddam, F. Hejabi, F. Heidari, S. Quazi and B. Farasati Far, *Med. Oncol.*, 2022, **39**, 240.

213 M. Gharbavi, S. Parvianian, M. P. Leilan, S. Tavangar, M. Parchianlou and A. Sharafi, *Nasal Drug Delivery: Formulations, Developments, Challenges, and Solutions*, 2023, pp. 279–324.

214 G. Parthasarathi, N. Udupa, P. Umadevi and G. Pillai, *J. Drug Targeting*, 1994, **2**, 173–182.

215 T. Liu and R. Guo, *Langmuir*, 2005, **21**, 11034–11039.

216 M. M. Mehanna, H. A. Elmaradny and M. W. Samaha, *Drug Dev. Ind. Pharm.*, 2010, **36**, 108–118.

217 E. Judy, M. Lopus and N. Kishore, *RSC Adv.*, 2021, **11**, 35110–35126.

218 R. Muzzalupo and L. Tavano, *Res. Rep. Transdermal Drug Delivery*, 2015, 23–33.

219 M. S. El-Ridy, S. A. Yehia, M. A.-E.-M. Kassem, D. M. Mostafa, E. A. Nasr and M. H. Asfour, *Drug Delivery*, 2015, **22**, 21–36.

220 Z. Ceren Ertekin, Z. Sezgin Bayindir and N. Yuksel, *Curr. Drug Delivery*, 2015, **12**, 192–199.

221 D. Kaur and S. Kumar, *J. Drug Delivery Ther.*, 2018, **8**, 35–43.

222 M. G. Umbarkar, *Indian J. Pharm. Educ. Res.*, 2021, **55**, 1–14.